

AD-A09d 107

ZEGAR-ABRAMS INC CLENSIDE PA  
HIGH POWER BROADBAND CANCELLATION SYSTEM.(U)  
MAR 81 L D WISMER, B S ABRAMS

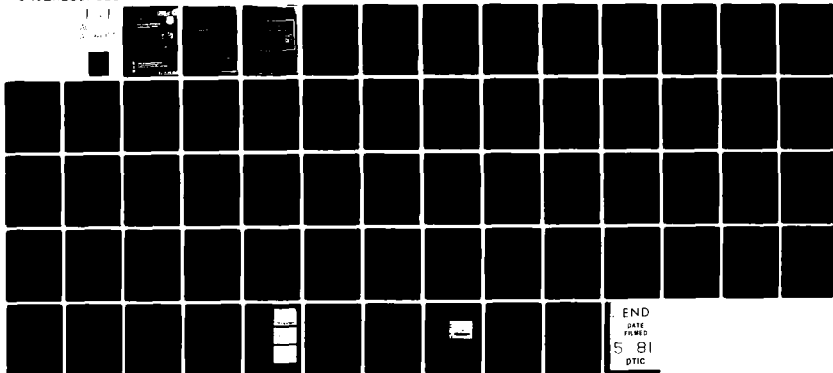
F/G 9/5

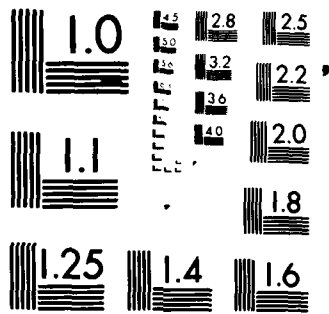
UNCLASSIFIED

RADC-TR-81-15

F30602-79-C-0180

NL





MICROCOPY RESOLUTION TEST CHART  
NATIONAL BUREAU OF STANDARDS 1963-A

AD A098107

THE UNITED STATES OF AMERICA  
DEPARTMENT OF THE ARMY  
OFFICE OF THE CHIEF OF STAFF  
WASHINGTON, D. C.

*Walter B. H. H. H.*  
WALTER B. H. H. H.  
WALTER B. H. H. H.

*W. B. H. H. H.*  
W. B. H. H. H.  
W. B. H. H. H.

*W. B. H. H. H.*  
W. B. H. H. H.  
W. B. H. H. H.

W. B. H. H. H.  
W. B. H. H. H.  
W. B. H. H. H.



UNCLASSIFIED

SECURITY CLASSIFICATION OF THIS PAGE (When Data Entered)

19 REPORT DOCUMENTATION PAGE		READ INSTRUCTIONS BEFORE COMPLETING FORM
1. REPORT NUMBER RADCR-81-15	2. GOVT ACCESSION NO. AD-A098107	3. RECIPIENT'S CATALOG NUMBER
4. TITLE (and Subtitle)	5. TYPE OF REPORT & PERIOD COVERED Final Technical Report 15 May 79 - 30 Oct 80	6. PERFORMING ORG. REPORT NUMBER N/A
7. AUTHOR(s) Lee D. Wismer Burton S. Abrams	8. CONTRACT OR GRANT NUMBER(s) F30602-79-C-0180	9. PROGRAM ELEMENT, PROJECT, TASK AREA & WORK UNIT NUMBERS 62702F 23380408
10. PERFORMING ORGANIZATION NAME AND ADDRESS Zeger-Abrams Incorporated 29 E. Glenside Ave Glenside PA 19038	11. CONTROLLING OFFICE NAME AND ADDRESS Rome Air Development Center (RBCT) Griffiss AFB NY 13441	12. REPORT DATE March 1981
13. MONITORING AGENCY NAME & ADDRESS (if different from Controlling Office) Same	14. SECURITY CLASS. (of this report) UNCLASSIFIED	15. DECLASSIFICATION/DOWNGRADING SCHEDULE N/A
16. DISTRIBUTION STATEMENT (of this Report) Approved for public release; distribution unlimited.		
17. DISTRIBUTION STATEMENT (of the abstract entered in Block 20, if different from Report) Same		
18. SUPPLEMENTARY NOTES RADCR Project Engineer: Wayne E. Woodward (RBCT)		
19. KEY WORDS (Continue on reverse side if necessary and identify by block number) Interference Cancellation UHF Communications Electromagnetic Compatibility		
20. ABSTRACT (Continue on reverse side if necessary and identify by block number) This report documents the effort on Contract F30602-79-C-0180 for Rome Air Development Center. The objective is to improve the broadband cancellation technology associated with adaptive UHF (225-400 MHz) Interference Cancellation Systems (ICS) employed with tunable or hopping transmitters. More specifically, the objective is to cancel a narrow-band transmitter waveform centered at a frequency $f$ plus its noise and modulation sidebands that extend over 0.02 % of $f_0$ . (Cont'd)		

DD FORM 1 JAN 73 1473 EDITION OF 1 NOV 65 IS OBSOLETE

UNCLASSIFIED

SECURITY CLASSIFICATION OF THIS PAGE (When Data Entered)

394516

UNCLASSIFIED

SECURITY CLASSIFICATION OF THIS PAGE(When Data Entered)

This report describes the concept for a two-channel ICS which provides improved broadband cancellation compared to that achievable with a single-channel ICS. The input to the second-channel weight is spectrally pre-shaped by an adaptive notch filter which automatically tracks the frequency of the interference. Control of the second-channel weight utilizes a novel pilot-directed control system.

A functioning unit was constructed to implement the design concept. Experimental measurements of the unit's performance across the 225 to 400 MHz band are presented which show  $f_0$  cancellation averaging about 60 dB, and sideband cancellation (at  $f_0 \pm 85$  KHz) averaging almost 55 dB. The settling time is less than 20 milliseconds. Suggestions for design refinements and for more extensive testing of the unit are discussed.

sub plus on minus



UNCLASSIFIED

SECURITY CLASSIFICATION OF THIS PAGE(When Data Entered)

## TABLE OF CONTENTS

Section	Page
1.0 INTRODUCTION AND SUMMARY	1
2.0 SYSTEM CONCEPT	3
2.1 Theory of Operation	3
2.2 System Design	7
3.0 SYSTEM IMPLEMENTATION	16
3.1 Block Diagram Description	16
3.2 Circuit Descriptions	21
4.0 OPERATING NOTES	44
5.0 SYSTEM PERFORMANCE	47
5.1 $f_o$ Cancellation	47
5.2 Sideband Cancellation	49
5.3 Acquisition Time	53
6.0 CONCLUSIONS AND RECOMMENDATIONS	56
REFERENCES	57

Accession For		
NTIS GRA&I	<input checked="" type="checkbox"/>	
DTIC TAB	<input type="checkbox"/>	
Unannounced	<input type="checkbox"/>	
Justification		
By		
Distribution/		
Availability Codes		
Avail and/or		
Dist	Special	
A		

## EVALUATION

The objective of this effort was to improve the high power broadband cancellation technology associated with adaptive interference cancellation systems employed on tunable or hopping transmitters. Reduction of close-in transmitter noise will permit closer assignment of transmitter and receiver frequencies on a collocated environment, such as an aircraft.

The significance of this effort is that the technology incorporated in the breadboard model is not singly limited only to cancelling close-in transmitter noise but can also be used as a test unit to determine its feasibility to cancel a complex multipath signal, and may also be usable to cancel a nonlinear interfering signal.

*Wayne E. Woodward*

WAYNE E. WOODWARD  
Project Engineer

## 1.0 INTRODUCTION AND SUMMARY

This final technical report describes the results obtained by Zeger-Abrams Incorporated on Contract F30602-79-C-0180 for Rome Air Development Center. The objective of this effort is to improve the broadband cancellation technology associated with adaptive UHF (225-400 MHz) Interference Cancellation Systems (ICS) employed with tunable or hopping transmitters. More specifically, the objective is to cancel a narrowband transmitter waveform centered at a frequency  $f_o$  plus its noise and modulation sidebands that extend over  $\pm 0.02\%$  of  $f_o$ .

This report describes the two-channel ICS concept developed by Zeger-Abrams to solve this problem. The first channel is a single-loop ICS which cancels the strong  $f_o$  component of the interference. Operating alone, it would leave residual sideband interference due to the unavoidable congruency mismatch between the channel and the antenna coupling path. The second ICS channel acts to cancel this sideband residue. It is able to do this because its input has been spectrally pre-shaped by a notch filter centered at  $f_o$ . The notch filter is implemented adaptively as an auxiliary single-loop ICS with one input delayed by the amount required to set the notch bandwidth. Having an adaptive notch filter means that the filter will automatically track changes in the interference center frequency  $f_o$ .

A pilot-directed control system is used with the second ICS channel. Low-level pilot sidebands are added to the output of the interfering transmitter. These provide a deterministic, constant-power reference which enables the second-channel control to operate much more effectively than it could using just the weaker transmitter noise sidebands as a reference.

This report also describes the embodiment of these design concepts into a broadband interference cancellation system (BBICS) breadboard model. Experimental results are presented to document the performance of the BBICS unit. Across the 225 to 400 MHz band,  $f_o$  cancellation averaging about 60 dB

and sideband cancellation (at  $f_0 \pm 85$  KHz) averaging almost 55 dB were observed. The settling time is less than 20 milliseconds. Suggestions for design refinements in the BBICS system and for more extensive testing of the unit are discussed.

## 2.0 SYSTEM CONCEPT

### 2.1 Theory of Operation

#### 2.1.1 Adaptive Interference Cancellers

Interference Cancellation Systems (ICS) adaptively protect a receiving antenna from interference caused by radiation from a co-located transmitter. A block diagram of an ICS is given in Figure 2.1.

The ICS operates by automatically adjusting the amplitude and phase of a sample of the transmitter waveform (reference) in a complex weight, whose output is combined with the receiving antenna output to effect cancellation of the transmitter waveform. Cancellation is maintained by a feedback control system which uses a sample of the ICS output as a feedback error signal which is correlated with the reference signal, amplified and lowpass filtered to drive the complex weight toward minimization of the feedback error signal [1].

The transmitter waveform can be conceptually separated into two components, both of which interfere with reception. The first component, the  $f_0$  component, is by far the strongest, but it is also spectrally confined and easier to cancel. The second component is noise sidebands, which are much weaker and more spectrally spread. The objective of this effort is to cancel the noise components over a  $\pm 0.02\%$  bandwidth by 60 dB while cancelling the  $f_0$  component by 65 dB. Thus, the problem involves broadband cancellation as well as cancellation of a high power  $f_0$  component.

#### 2.1.2 Limits on Broadband Cancellation

Deep cancellation of a broadband transmitted waveform requires congruency between the reference path and the interference coupling path. By requiring congruency we mean that the phase and amplitude characteristics of the two paths must track one another over the frequency band of interest. Frequency-invariant differences will be adjusted by the complex weight, leaving the frequency-varying differences as the principal cancel-

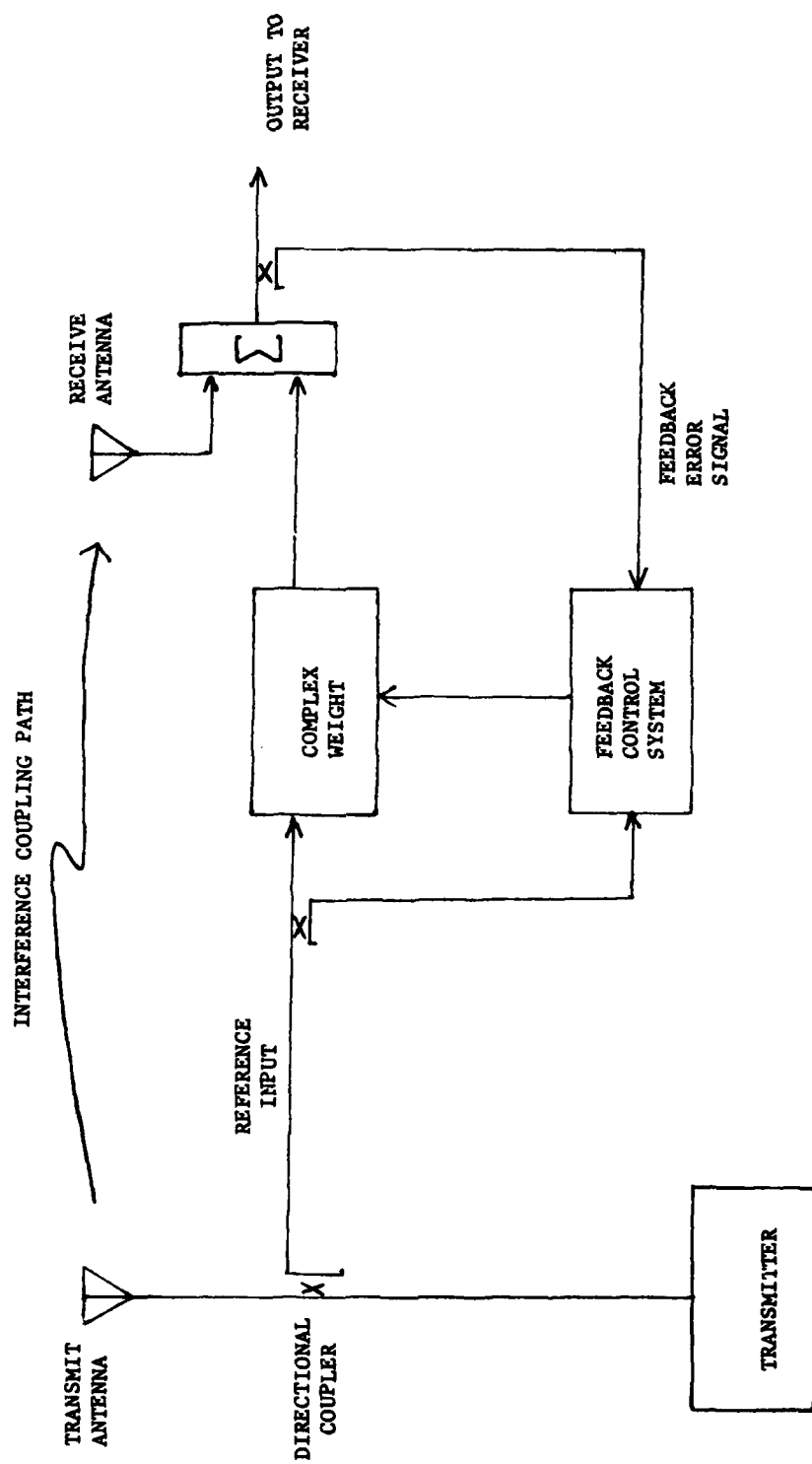


Figure 2.1 Adaptive Interference Canceller - Basic Block Diagram

lation limitation.

There are a number of factors that contribute to these amplitude and phase mismatches. They include differential time delay through the two paths, frequency-dependent variations in system components, and multipath effects.

### 2.1.3 Channel Equalization to Overcome Broadband Cancellation Limits

The reference path and the interference coupling path may be thought of as two channels with slight differences in their amplitude and phase characteristics. Differences in amplitude and phase that are frequency independent are easily corrected by a wideband complex weight. Frequency dependent differences need higher order compensation in the form of channel equalization to assure good cancellation of interferences.

Channel equalizers have most commonly taken the form of sampled data filters either of the transversal type or of the recursive type [2]. The transversal filter consists of a cascade of time delays, the outputs of which are individually weighted and combined in a feed-forward configuration. The recursive filter consists of a cascade of delays, the outputs of which are individually weighted and combined in a feedback configuration.

Channel equalizers, however, need not be restricted to cascading time delays. Other networks may also be cascaded, including notch filters [3]. Figure 2.2 shows a cascade of notch filters, each of whose outputs are individually weighted and then combined. Each notch filter in the cascade contributes a term to the series expansion that approximates the channel. This series converges rapidly as long as the rate of change of the channel characteristics is much smaller than the reciprocal bandwidth of the signals, which is the case for the ICS. Rapid convergence of the series means that for each additional notch filter and weight, the approximation error (the output residue) is greatly reduced.

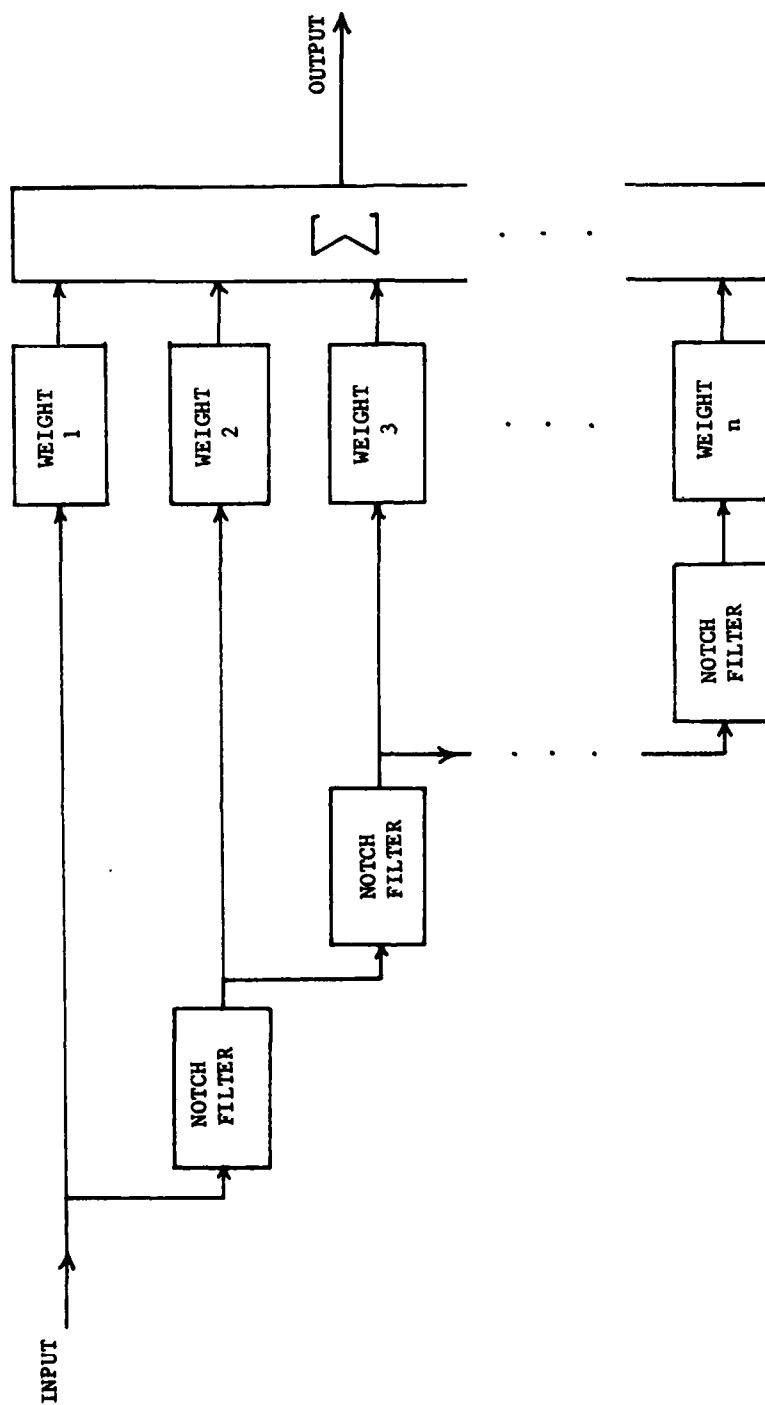


Figure 2.2 Channel Equalizer Using Cascaded Notch Filters

## 2.2 System Design

The design approach selected for the BBICS system, illustrated in Figure 2.3, embodies the first two terms of the notch filter cascade of Figure 2.2. The reference input is split into two portions. One portion goes directly to a complex weight, the other is first notch filtered, then weighted. The weighted references are combined with the signal from the receive antenna to produce the cancelled output to the receiver. A sample of the cancelled output is extracted through a directional coupler to provide a feedback error signal to the adaptive control unit. The adaptive control adjusts both weights for maximum broadband cancellation.

### 2.2.1 Adaptive Notch Filter

The notch filter will be implemented adaptively, as shown in Figure 2.4. We represent the input and output signals by their Fourier transforms,  $S_i(f)$  and  $S_o(f)$  respectively. The  $\tau$ -second delay line has a transfer function  $e^{-j2\pi f\tau}$ .

The LMS (Least Mean-Square) algorithm [4] for adaptive control is used, wherein a sample of the input to the weight (reference) is correlated with a sample of the cancelled output (error), and the result of this correlation is integrated to produce the weight value. In practical applications, a lowpass filter with a long time constant would replace the ideal integrator.

If the input signal has a strong fundamental component at  $f_o$ , the LMS control will adjust the complex weight to have the value  $-e^{-j2\pi f_o\tau}$ , so that the transfer function of the filter (including the 3 dB losses in the hybrids) becomes:

$$H(f) = \frac{S_o(f)}{S_i(f)} = \frac{1}{2} \left( e^{-j2\pi f\tau} - e^{-j2\pi f_o\tau} \right) \quad (2.1)$$

Note that  $H(f) = 0$  for  $f = f_o$ , implying perfect cancellation at the center frequency, which is expected for an ideal notch filter. The magnitude

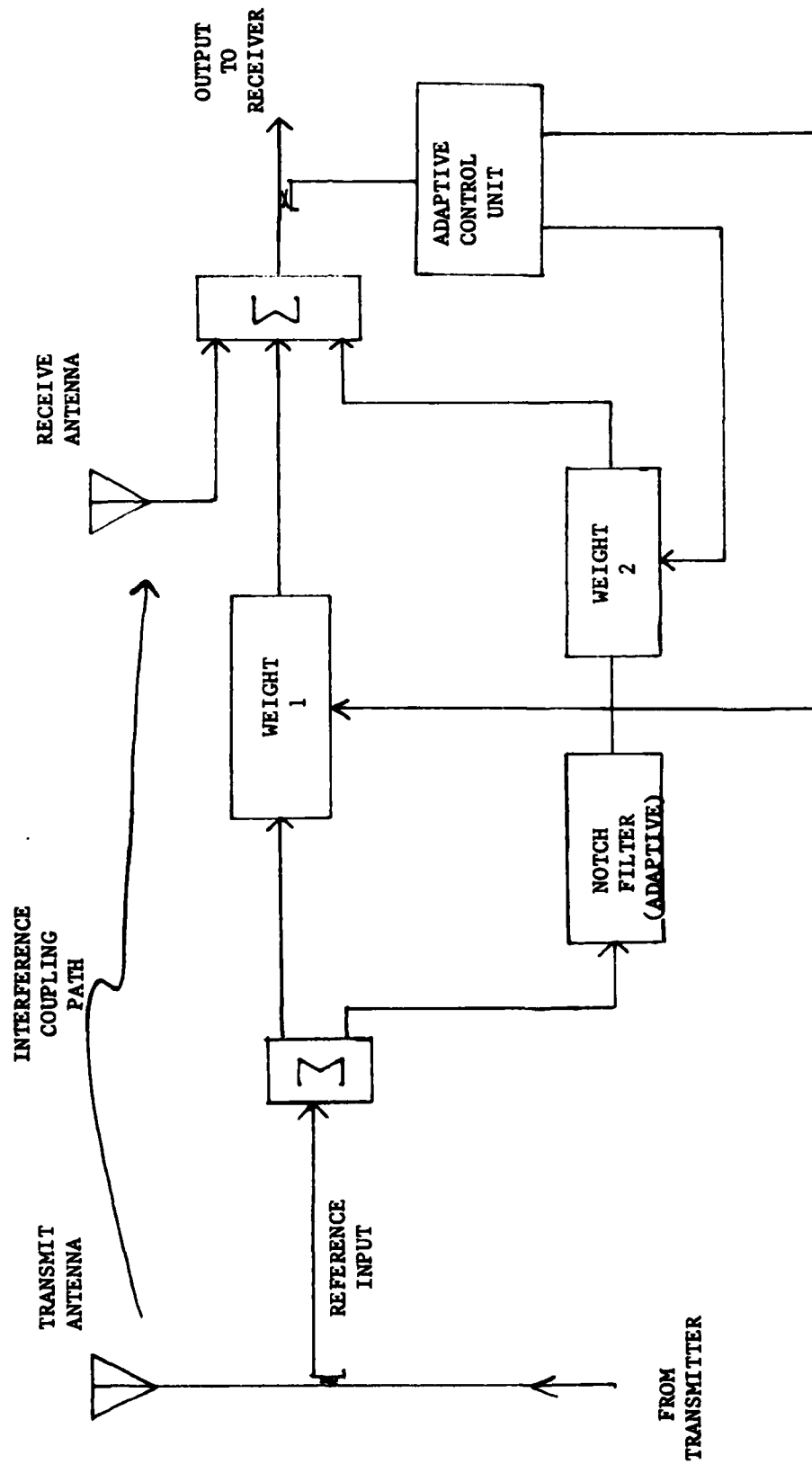


Figure 2.3 BBICS System Design

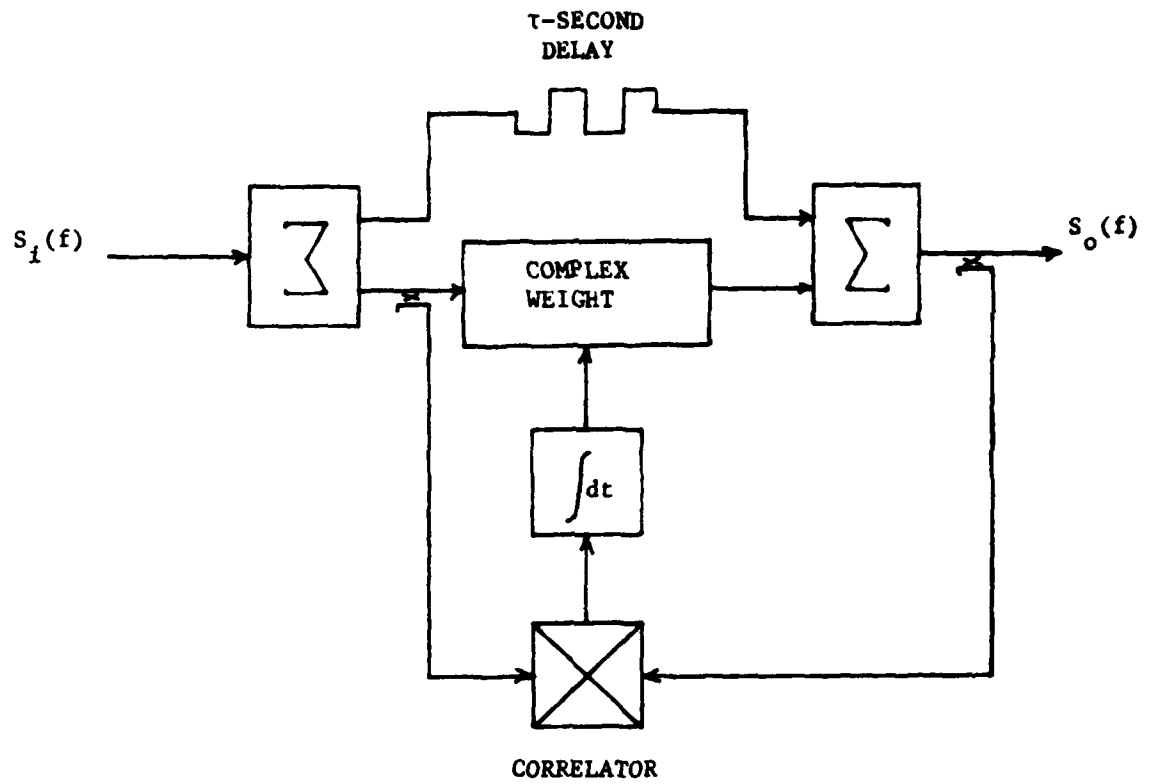


Figure 2.4 Adaptive Notch Filter Block Diagram

and phase of the transfer function are found to be:

$$\begin{aligned} |H(f)| &= \sqrt{\frac{1}{2} - \frac{1}{2} \cos(2\pi\Delta f\tau)} \\ &= |\pi\Delta f\tau| \text{ for } 2\pi\Delta f\tau \ll 1 \end{aligned} \quad (2.2)$$

$$\text{Arg } [H(f)] = -\pi\Delta f\tau + \left(\frac{\pi}{2} - 2\pi f_o\tau\right) \quad (2.3)$$

where we have defined

$$\Delta f \equiv f - f_o \quad (2.4)$$

Plots of the magnitude and phase appear in Figure 2.5. Note from the approximation in (2.2) that the variation of  $|H(f)|$  with  $\Delta f$  is almost linear near  $f_o$ . If a narrow band-limited rectangular spectrum centered about  $f_o$  were passed through the filter, the magnitude of the output spectrum would be shaped like the letter M. This is the so-called M-effect, the characteristic manifestation of broadband cancellation limits in a single-channel ICS. Note also from the phase plot that, relative to the phase shift seen at the fundamental frequency  $f_o$ , the phase shifts encountered by two sidebands at  $+\Delta f$  and  $-\Delta f$  away from  $f_o$  will be equal and opposite. This effect will impact on the operation of the pilot sideband control system, to be discussed subsequently.

### 2.2.2 System Block Diagram

Based on the concept of Figure 2.3, a general system block diagram has been developed and is presented in Figure 2.6. The signal from the transmitter enters the Pilot Modulator before going to the transmit antenna. To simplify the explanation of system operation, it will be assumed that this transmitter signal is simply a sinusoid at frequency  $\omega_o$ , whose spectrum is a single impulse as shown. The Pilot Modulator is one element of a pilot-driven system being used to adaptively control the Sideband Weight. The general concept of a pilot-driven control has been described previously in [5]; the operation of the particular pilot system being used here will be explained shortly.

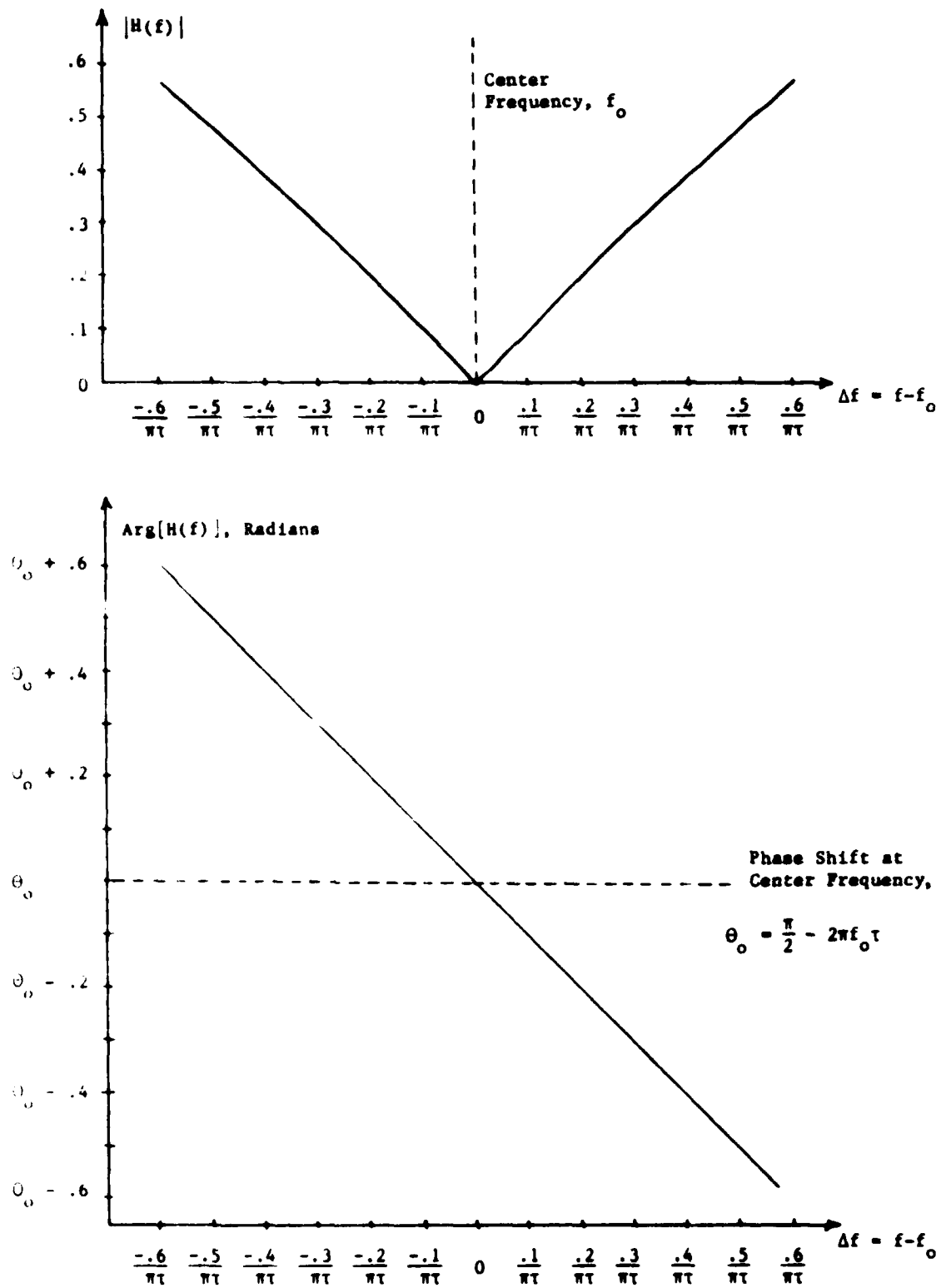


Figure 2.5 Magnitude and Phase Characteristics of the Adaptive Notch Filter Near  $f_0$

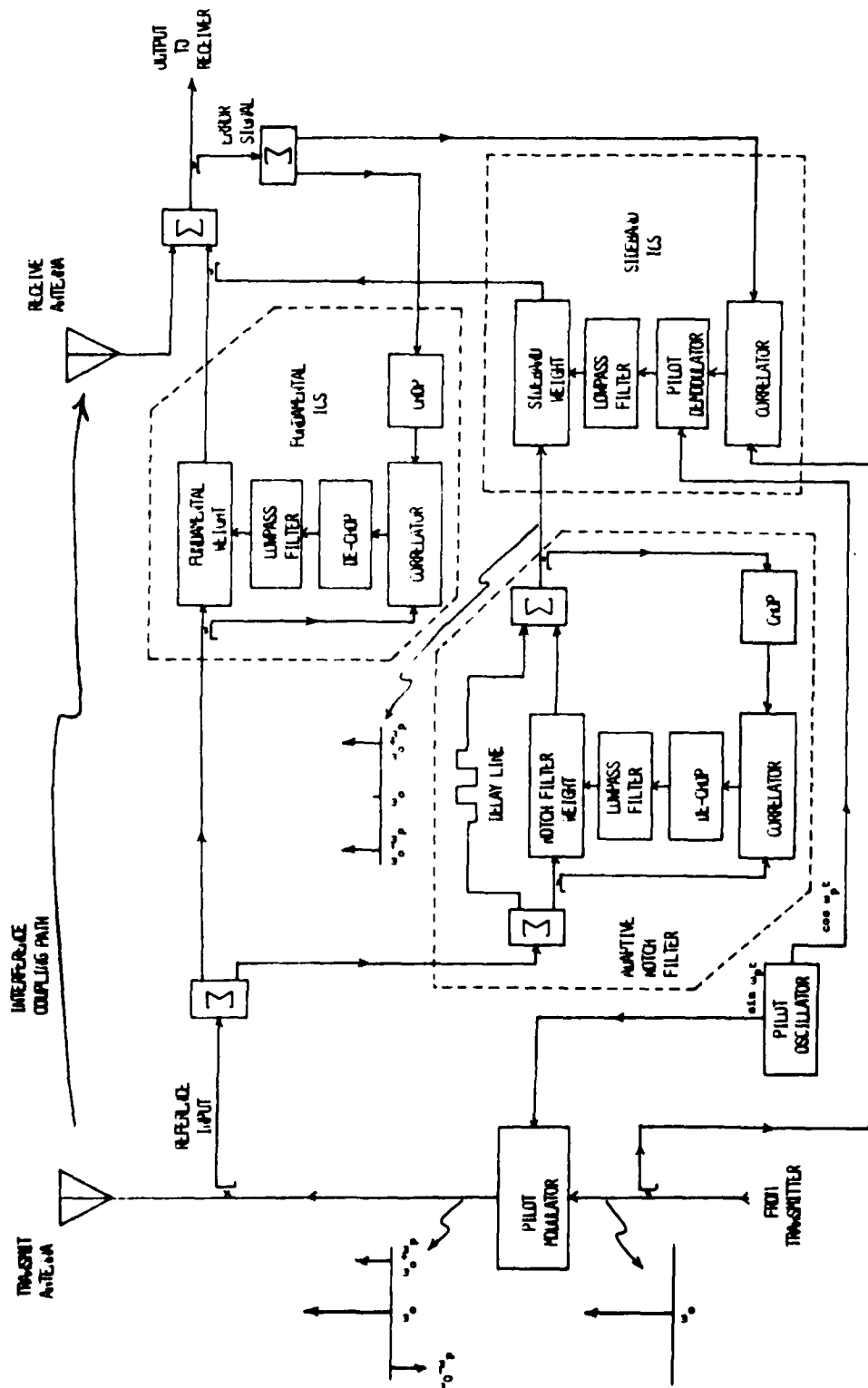


Figure 2.6 BBICS General System Block Diagram

The Pilot Modulator adds low-level sidebands to the transmitter waveform by modulating it against the  $\sin \omega_p t$  output of the Pilot Oscillator. Modulation against  $\sin \omega_p t$  (as opposed to  $\cos \omega_p t$ ) causes the sidebands to be out of phase with each other, as indicated in the spectrum shown. This output, consisting of the transmitter signal plus the pilot sidebands, is what gets broadcast from the transmit antenna.

The pilot sidebands can be thought of as partners to the transmitter noise sidebands that we desire to cancel. From the point where they are added to the transmitter waveform, the pilot sidebands undergo exactly the same processing as the noise sidebands. It follows that if the ICS can be made to cancel the pilot sidebands, the noise sidebands will automatically be cancelled as well. This is the underlying foundation of the pilot control system. Control of the ICS by the pilot sidebands is preferable to control by the noise sidebands, because the former are deterministic signals with a larger and constant reference power level.

The reference input to the system is split two ways: one half goes into the Fundamental ICS, the other into the Adaptive Notch Filter. The Fundamental ICS utilizes LMS adaptive control, which was described previously. A refinement of the control system places a chopper on the error signal ahead of the correlator. The use of a chopped error signal produces correlator outputs at the chopping frequency instead of at DC, thereby removing problems of DC drift and  $1/f$  noise. Correlators with DC outputs will not allow cancellation ratios as deep as 60 dB. The correlator outputs are subsequently restored to DC, after amplification at the chopping frequency, where they are lowpass filtered and amplified further. The lowpass filter outputs provide the control voltages for the complex weight.

The Fundamental ICS operates in the usual manner of a single-channel ICS, and does so independently of the other loops present. In fact, if the Adaptive Notch Filter and Sideband ICS subsystems were removed from Figure 2.6, the Fundamental ICS would still cancel the  $\omega_o$

component entering the receive antenna. But owing to the M-effect caused by incongruities between the interference coupling path and the fundamental reference input path, the pilot sidebands would not be sufficiently cancelled.

The Adaptive Notch Filter operates exactly as described in Section 2.2.1, except that chopping and de-chopping have been added to its control system. Like the Fundamental ICS, the Adaptive Notch Filter cancels the strong  $\omega_0$  component appearing at its input. But the pilot sidebands are cancelled very little, and appear in the spectrum of the filter output as shown. Note that the relative phase of the two sidebands has been inverted. This is due to the phase characteristics of the Notch Filter as was noted in Figure 2.5. This inverted-sideband spectrum is effectively what would result from modulating the  $\omega_0$  fundamental with  $\cos \omega_p t$  instead of  $\sin \omega_p t$ .

The objective of the system at this point is to control the Sideband Weight to adjust the magnitude and phase of the sideband spectrum that comes out of the Notch Filter in such a way that when it is combined with the Fundamental Weight output, it will act to cancel the residual sidebands that would be present if the Fundamental ICS were operating alone. The typical LMS control approach would be to correlate an error signal sampled from the system output with a reference signal sampled from the input to the Sideband Weight. But such a scheme would not work in a practical system, because imperfect cancellation leaves residual components at  $\omega_0$  in both of these signals that have power levels greater than the pilot sidebands. The correlator output would be dominated by the product of these fundamental components, rather than by the product of the sidebands as it should be.

A solution to this problem is the approach that Figure 2.6 illustrates. Instead of taking the correlator reference from the input to the Sideband Weight, it is taken from all the way back at the transmitter output, ahead of the Pilot Modulator. This correlates with any

uncancelled pilot sidebands in the error signal to produce a correlator output at the pilot frequency  $\omega_p$ . This correlator output is then brought down to DC in the Pilot Demodulator where it is synchronously detected against the output of the Pilot Oscillator. Because the Adaptive Notch Filter flips the relative phase of the sidebands, the  $\cos \omega_p t$  output, rather than the  $\sin \omega_p t$  output, must be used for detection. The detected signal is then lowpass filtered to produce the control voltage for the Sideband Weight.

The Sideband Weight output is combined with the Fundamental Weight output in a directional coupler to produce a least mean square estimate of the coupled interference waveform. Combining this estimate with the waveform from the receive antenna then produces at the output deep cancellation of  $\omega_o$  plus the pilot sidebands, implying deep cancellation of transmitter noise sidebands as well.

### 3.0 SYSTEM IMPLEMENTATION

A functioning system was built to implement the system concept discussed in the previous section. The system is housed in a standard 19" rack-mount chassis, and is designed to operate with a 33 dBm level reference input. There are five external RF connections to the chassis, all made through BNC connectors on the front panel. The layout of the front panel, showing the labelling of these connectors, is given in Figure 3.1. A cutaway top view of the system, showing the location of boxed subassemblies within the main chassis, is presented in Figure 3.2.

#### 3.1 Block Diagram Description

Figure 3.3 is a block diagram representation of the BBICS system. Operation of the system will be described with reference to this figure.

Signals from the transmitter enter the system through the "PILOT MODULATOR--RF IN" connector, which leads to a 20 dB directional coupler that extracts a sample of the transmitter waveform through the coupled path to provide a reference for the sideband ICS correlator. The straight-through path leads to the Pilot Modulator, Box P, Card 1, which adds low level 85 KHz pilot sidebands to the signal to be transmitted. The sidebands are produced by modulating a sample of the transmitter waveform with the  $\sin \omega_p t$  output of the Pilot Oscillator. The output of the Pilot Modulator is returned to the front panel at the "PILOT MODULATOR--RF OUT" terminal, which gets connected externally to the transmit antenna.

Somewhere between the terminal and the antenna, a 33 dBm sample of the transmitted signal, including pilot sidebands, must be extracted to provide the reference input for the system. This reference signal enters the system through the "REFERENCE INPUT" connector. The reference input is then split between the Fundamental ICS and the Adaptive Notch Filter by the TU-50 hybrid. The Fundamental ICS Weight, Box W1, Card 1, performs a complex (amplitude and phase) weighting on the reference input, and its output goes to the CR-10-500 coupler (10 dB). The Adaptive Notch

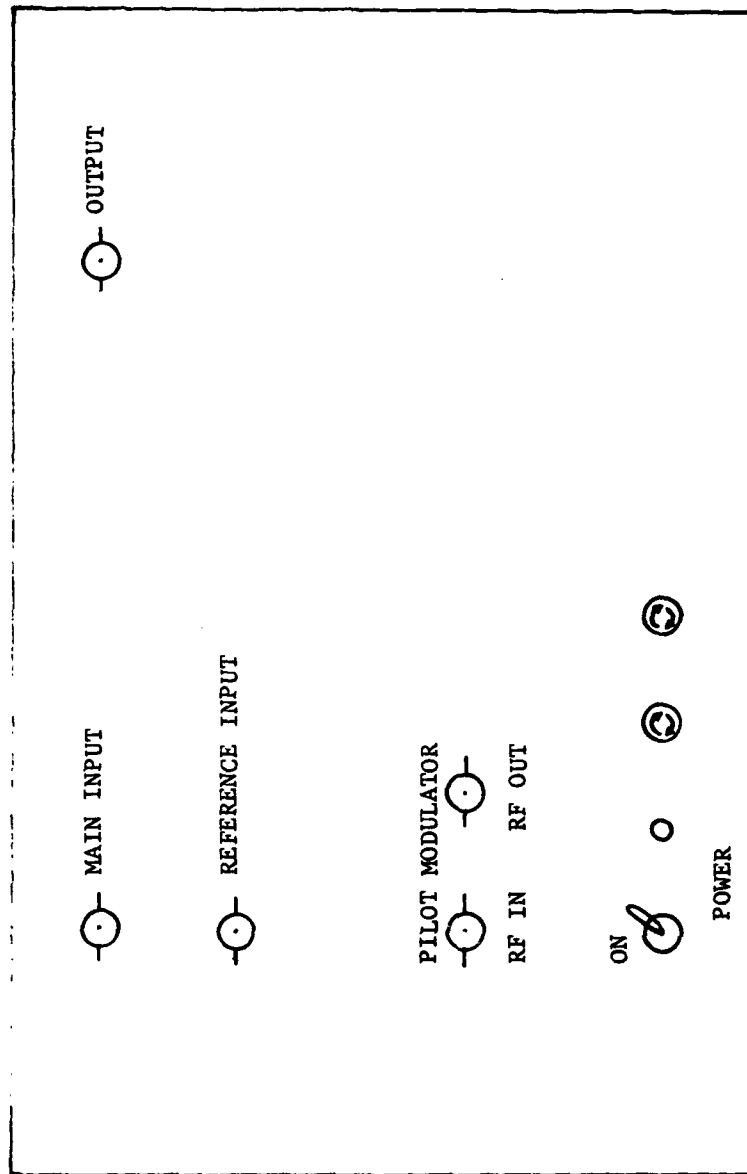
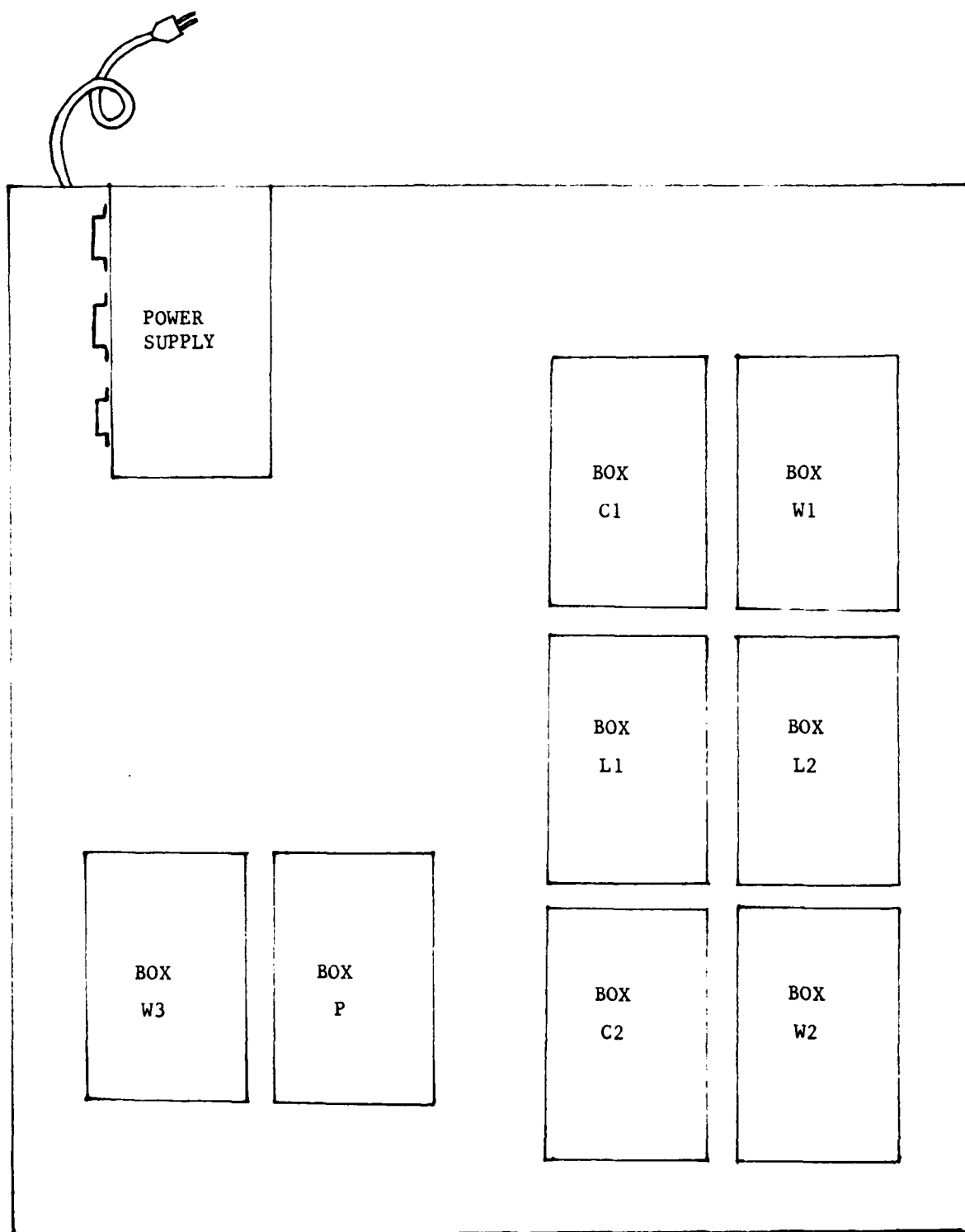


Figure 3.1 BBICS Front Panel Layout



FRONT PANEL

Figure 3.2 Cutaway Top View of BBICS Chassis

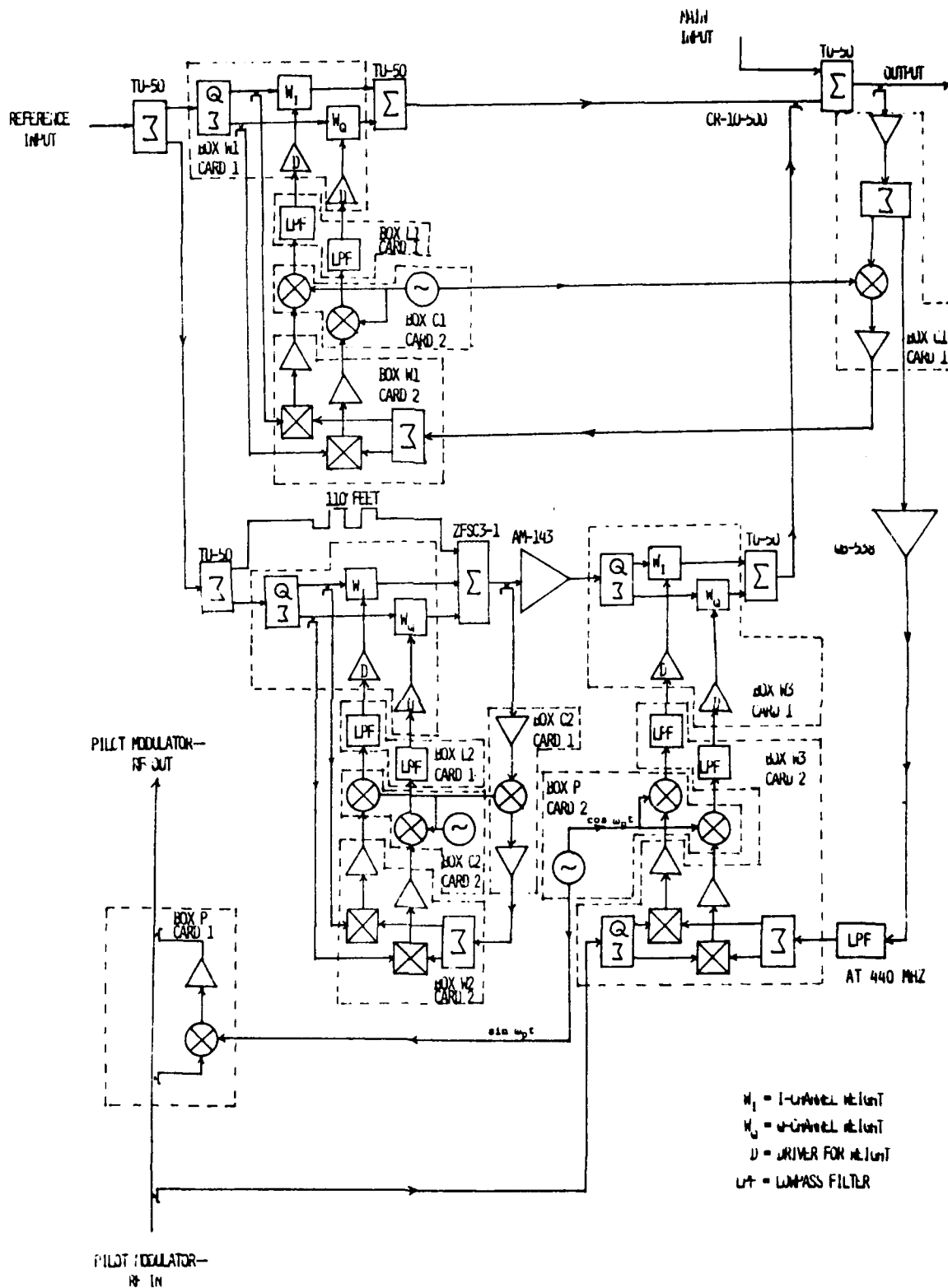


Figure 3.3 BBICS Detailed System Block Diagram

Filter contains a second TU-50 splitter which further divides the reference input between the Notch Filter Weight and the 110-foot delay line. The Notch Filter Weight, Box W2, Card 1, adjusts its reference input in amplitude and phase to cancel the large fundamental component in the delayed reference when they combine in the ZFSC3-1 hybrid. This creates an M-shaped spectrum which is amplified by the AM-143, then weighted by the Sideband ICS Weight, Box W3, Card 1.

The weighted M-spectrum is combined with the weighted fundamental reference at the CR-10-500 coupler. Cancellation takes place at the TU-50 hybrid where the input from the receive antenna, brought into the system through the "MAIN INPUT" connector, is combined with the weighted reference spectra. This cancelled output leaves the system via the "OUTPUT" terminal, which can be connected externally to a receiver (or a receive multicoupler).

A sample of the cancelled output is extracted by a 10 dB directional coupler to provide the error signal input to the ICS Error Signal Chopper, Box C1, Card 1. This card splits the error signal into two portions. One portion leaves the card, is amplified by the QB-538, and provides the error input to the Sideband ICS Correlator. The other portion is chopped at 10 KHz and amplified to provide the chopped error input to the Fundamental ICS Correlator. The 10 KHz chopping signal is brought in from the oscillator in Box C1, Card 2.

The Fundamental ICS Correlator, Box W1, Card 2, performs the complex correlation between a sample of the reference input, tapped off just ahead of the Fundamental Weight, and the chopped error signal. The correlator outputs are at the chop frequency, 10 KHz, and are amplified and bandpass filtered to reject harmonics of the chop frequency.

De-chopping of the Fundamental Correlator outputs takes place in Box C1, Card 2. The de-chopped control signals are lowpass filtered and amplified in Box L1, Card 1. The corner frequency of the LPF is .034 Hz. Finally, the filtered control signals go to Box W1, Card 1, where they

control the drivers for the Fundamental Weight.

The control system for the Adaptive Notch Filter operates identically. A sample of the Notch Filter output is extracted by a 10 dB directional coupler and chopped at 10 KHz in the Notch Filter Chopper, Box C2, Card 2. The other correlator input is the reference input sample, tapped off the input to the Notch Filter Weight. The correlator output is de-chopped in Box C2, Card 2, lowpass filtered in Box L2, Card 1, and the resulting control signals go to the Notch Filter Weight drivers in Box W2, Card 1.

The control system for the Sideband ICS operates differently, owing to the use of the pilot sidebands to control its weight. The inputs to the Sideband ICS Correlator, Box W3, Card 2, are the amplified error signal from Box C1, Card 1, which contains any uncanceled residue of the pilot sidebands, and the reference input from the transmitter, tapped off ahead of the Pilot Modulator and therefore free of pilot sidebands. The correlator output is at the pilot frequency, 85 KHz. In the Pilot Demodulator, Box P, Card 2, this correlator output is synchronously detected against the  $\cos \omega_p t$  output of the Pilot Oscillator. The detected signals return to Box W3, Card 2, for lowpass filtering, and the filtered control signals go to the drivers for the Sideband Weight, Box W3, Card 1.

### 3.2 Circuit Descriptions

#### 3.2.1 Box W1

The connections to Box W1 are listed in Table 3.1. The terminals used for +15 and -15 volt supplies are 1500 pf feed-through connectors, to prevent RF pick-up on these lines from entering or exiting the box. All connections are on the box lid.

Table 3.1  
Connections to Box W1

Signal	Type of Connector
Reference In	BNC
Chopped Error In	BNC
Weighted I Out	BNC
Weighted Q Out	BNC
+15 Volts	1500 pf feed through
-15 Volts	1500 pf feed through
I 10 KHz Out	Multipin connector, Pin F
Q 10 KHz Out	Multipin connector, Pin E
I <sup>+</sup> Control In	Multipin connector, Pin D
I <sup>-</sup> Control In	Multipin connector, Pin K
Q <sup>+</sup> Control In	Multipin connector, Pin C
Q <sup>-</sup> Control In	Multipin connector, Pin H
Gnd	Multipin connector, Pin B

#### 3.2.1.1 Card 1: Fundamental ICS Weight and Driver

Figure 3.4 shows the schematic diagram for this card. The complex weight is implemented as two real balanced modulators in quadrature. The reference input enters the box through a BNC connector on the lid, and proceeds to the 1A0260-3 quadrature hybrid, where it is split into I and Q components. From this point on, processing of the I and Q channels is identical. Therefore, Figure 3.4 shows only the I-side circuitry. The 20 dB directional coupler (PDC20-1) taps off a fraction of the I (or Q) waveform through its coupled port to provide a reference for the Fundamental Correlator. The straight-through port leads into a PIN diode bridge balanced modulator. Two UM4301B PIN diodes in series are used in each leg of the bridge to provide low intermodulation distortion. The weighted I and Q waveforms leave the box through BNC connectors on the lid, and they are recombined in a TU-50 hybrid attached to the side of the box.



The driver circuitry controls the bias current applied to the PIN diodes. The active elements in the drive are 2N6659 VMOSFETs, chosen for their ability to provide moderately high drive currents with low noise. The drivers respond to the control inputs  $I^+$  and  $I^-$  for the I channel and  $Q^+$  and  $Q^-$  for the Q channel. The system has been designed for symmetrical control signals; that is,  $I^+ = -I^-$  and  $Q^+ = -Q^-$ . The diode networks at the source of each MOSFET compensate for control nonlinearities inherent in the characteristics of the MOSFETs and the PIN diodes, making the RF output voltage response of the combined modulator and driver very nearly linear with respect to the input control voltage.

#### 3.2.1.2 Card 2: Fundamental ICS Correlator and 10 KHz Amplification

The schematic diagram for the I-channel circuitry is presented in Figure 3.5. The Q-side circuit is identical. The correlator is implemented as a diode quad double-balanced mixer, with a small DC bias current applied to the diodes to maintain linearity with respect to both inputs without sacrificing sensitivity at low input levels. The two inputs to the correlator are: the I (or Q) reference input, which is attenuated 10 dB before entering the correlator; and the chopped error signal, which the PSC2-1 hybrid splits between the I and Q correlators.

The correlator output is at the chop frequency, 10 KHz. The 2N930 low noise transistor stage amplifies this 10 KHz signal by about 16 dB. The transistor output is buffered through the 747 op amp in unity gain configuration, then amplified further by the 715 op amp. The 715 is configured as a bandpass filter at 10 KHz, to eliminate harmonics of the chop frequency.

#### 3.2.2 Box C1

Table 3.2 lists the connections to Box C1. All connections are on the box lid. Feed-through connectors (1500 pf) are used for the +15 and -15 volt supply lines, 10 KHz I and Q lines, and de-chopped I and Q lines to prevent RF pick-up on these lines from entering or exiting the box.



### Figure 3.5 Box W1, Card 2: Fundamental ICS Correlator and 10 KHz Amplification

Table 3.2  
Connections to Box C1

Signal	Type of Connector
Error In	SMA
Chopped Error Out	BNC
Unchopped Error Out	BNC
I 10 KHz In	1500 pf feed-through
Q 10 KHz In	1500 pf feed-through
De-chopped I Out	1500 pf feed-through
De-chopped Q Out	1500 pf feed-through
+15 Volts	1500 pf feed-through
-15 Volts	1500 pf feed-through

#### 3.2.2.1 Card 1: ICS Error Signal Chopper

As shown in the schematic diagram in Figure 3.6, the error signal entering the box is first amplified 14 dB by the MWA-120. The PSC2-1 hybrid splits the amplified error signal between two paths: One is used for control of the Fundamental ICS, the other for control of the Sideband ICS. The latter receives no further processing and leaves the box through a BNC connector in the lid. The former enters the SRA-1 mixer to be chopped. The chopping is simply a double-sideband (DSB) modulation of the error signal by a 10 KHz chopping signal. This 10 KHz signal is generated on Card 2 of this box, and is applied to the IF port of the mixer through the CD40107B driver.

The chopped signal is amplified further by the A75, whose output is limited by the presence of the Shottky diodes. Too large an output signal from the A75, as might occur during acquisition of the ICS, could overdrive the correlator to which this signal is sent.

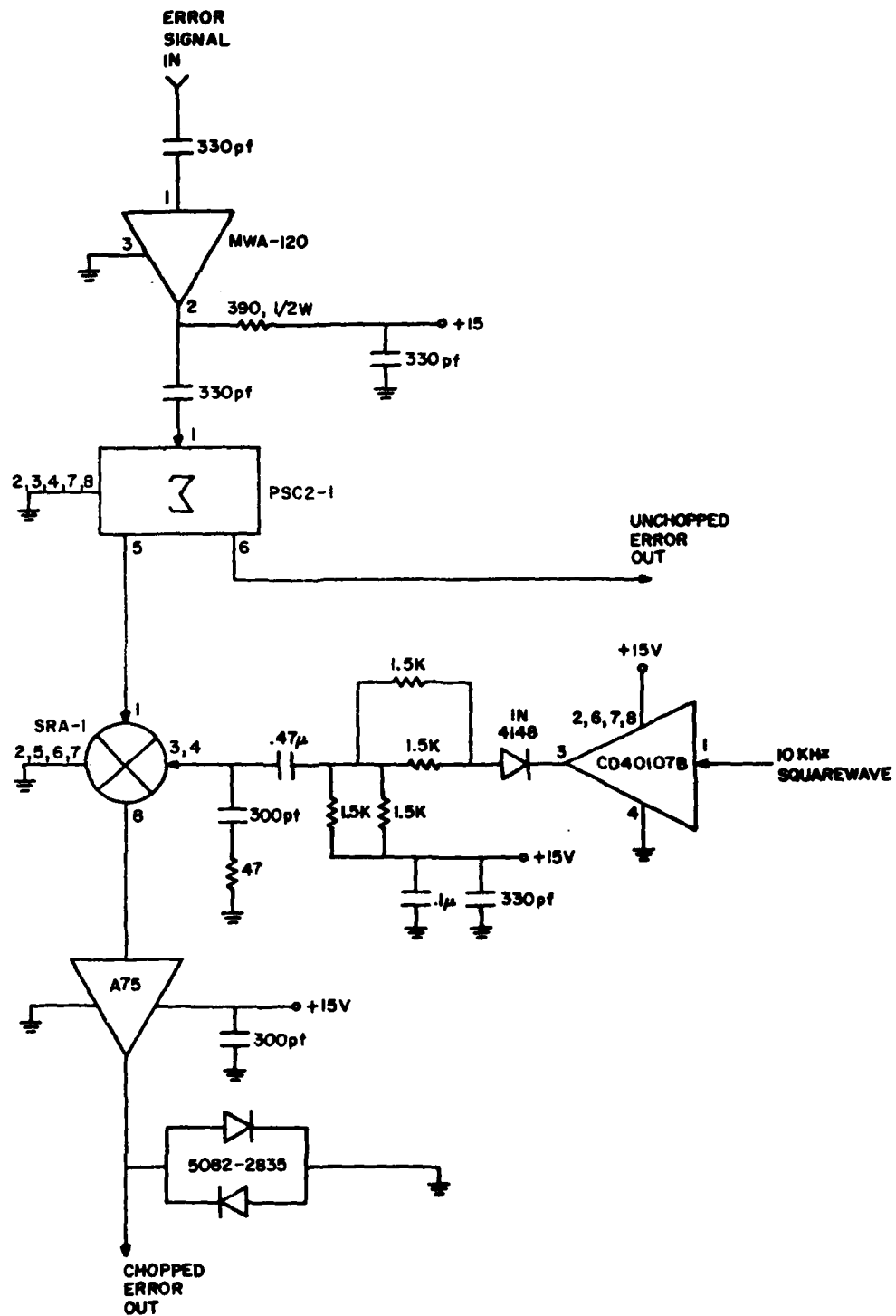


Figure 3.6 Box C1, Card 1: ICS Error Signal Chopper

### 3.2.2.2 Card 2: Fundamental ICS 10 KHz Generation and De-chopping

Figure 3.7 shows the schematic diagram for this card. The 10 KHz chopping signal is the square-wave output of the CD4047B oscillator. The de-chopper is actually a full-wave synchronous detector at the chop frequency implemented with the DG300 analog switch and the 747 op amps. The switch, controlled by the 10 KHz square wave, alternately flips the op amp configuration between inverting unity-gain and non-inverting unity-gain modes.

### 3.2.3 Box L1

Table 3.3 lists the connections to Box L1. All connections are on the lid. No RF signals are processed in this box.

Table 3.3  
Connections to Box L1

Signal	Type of Connector
De-chopped I In	Multipin connector, Pin F
De-chopped Q In	Multipin connector, Pin E
$I^+$ Control Out	Multipin connector, Pin D
$I^-$ Control Out	Multipin connector, Pin K
$Q^+$ Control Out	Multipin connector, Pin C
$Q^-$ Control Out	Multipin connector, Pin H
+15 Volts	Multipin connector, Pin A
-15 Volts	Multipin connector, Pin J
Gnd	Multipin connector, Pin B

#### 3.2.3.1 Card 1: Fundamental ICS Lowpass Filtering

Box L1 contains only this single card, whose schematic is shown in Figure 3.8. Only I-channel circuitry is shown, since the Q-channel is identical. The de-chopped I (or Q) control signal enters the first HA4741

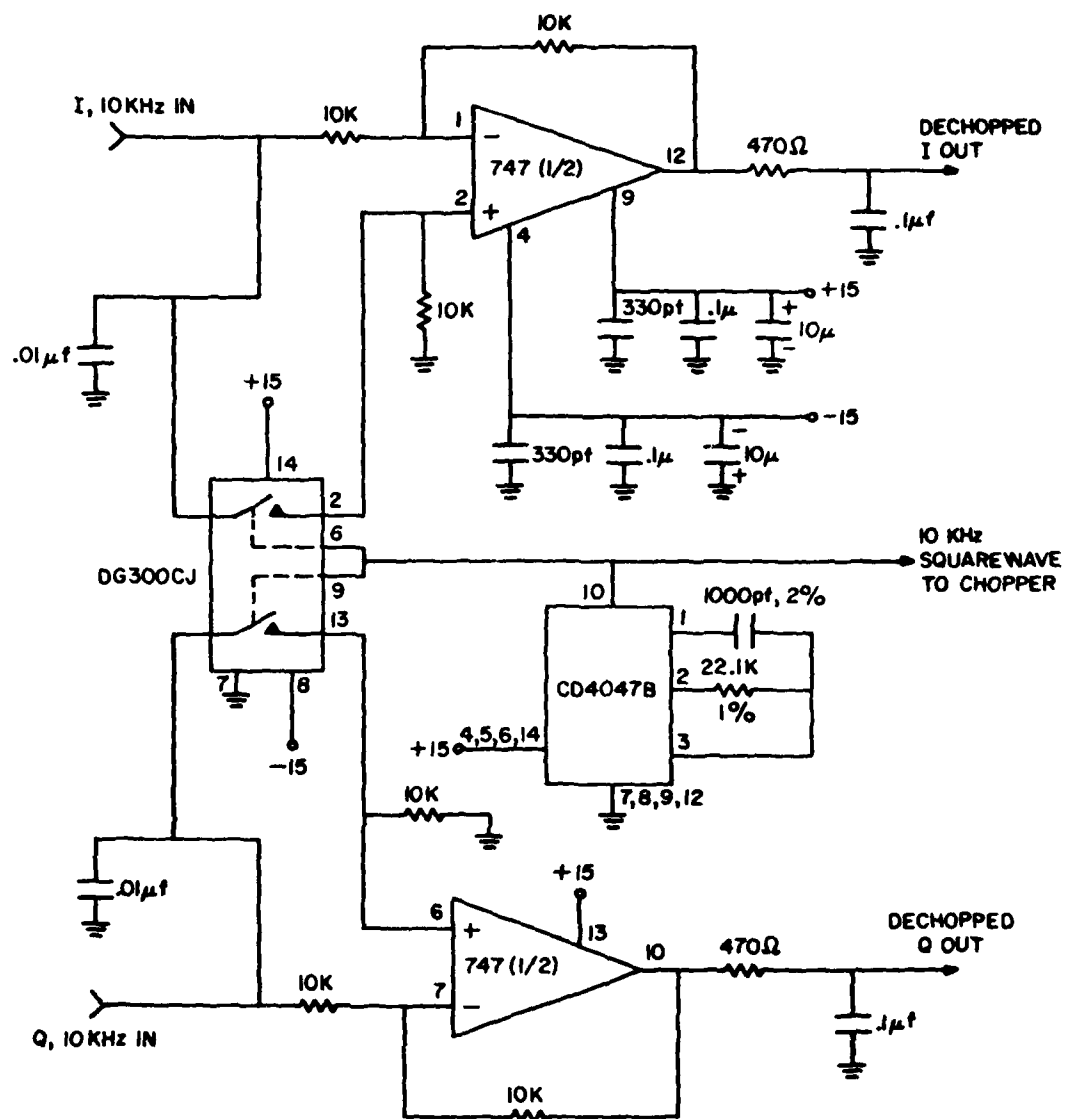


Figure 3.7 Box C1, Card 2: Fundamental ICS 10 KHz Generation and De-chopping

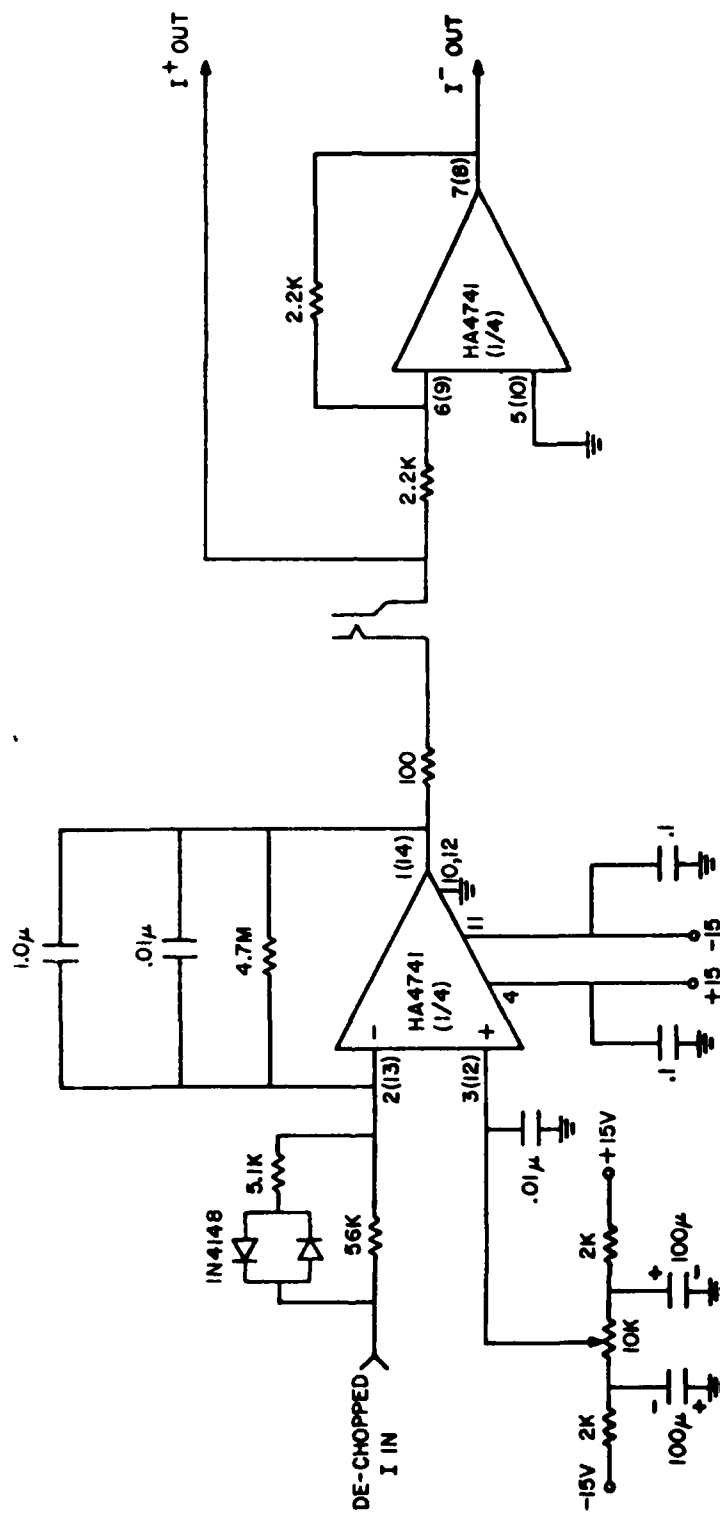


Figure 3.8 Box L1, Card 1: Fundamental ICS Lowpass Filtering

op amp, configured as a .034 Hz lowpass filter with a normal DC gain of 38 dB.

When the voltage drop across the 56 K input resistor exceeds .7 volts, one of the parallel diodes will switch on and reduce the effective input resistance, which in turn increases the DC gain of the LPF. This typically occurs during acquisition of the loop, and the increased gain allows the loop to acquire more quickly. After acquisition, the input voltages will be at levels well below .7 volts, and the diodes remain turned off. The 10 K pot can be adjusted to compensate for DC offsets in the de-chop and LPF op amps. The large 100  $\mu$ f decoupling capacitors on the +15 and -15 volt ends of the pot are necessary to prevent 60 Hz power supply ripple from getting on the control lines.

Jacks are provided at the LPF outputs for diagnostic purposes. They enable manual control of the weight by the application of external control voltages, or they can be used to monitor control voltages during automatic operation. The LPF output appearing at the jack represents the  $I^+$  (or  $Q^+$ ) control signal. The unity-gain HA4741 stage which follows inverts this signal to provide the  $I^-$  (or  $Q^-$ ) signal for symmetric control.

#### 3.2.4 Box W2

This box is identical in construction to Box W1. See Section 3.2.1 and Table 3.1.

##### 3.2.4.1 Card 1: Adaptive Notch Filter (ANF) Weight and Driver

This card is identical to Box W1, Card 1. See Section 3.2.1.1 and Figure 3.4.

##### 3.2.4.2 Card 2: ANF Correlator and 10 KHz Amplification

This card is identical to Box W1, Card 2. See Section 3.2.1.1 and Figure 3.5.

#### 3.2.2.1 Box C2

Table 3.4 lists the connections to Box C2, all of which are on the lid. Once again, 1500 pf feed-through connectors are used for the +15 and -15 volt supply lines, 10 KHz I and Q lines, and de-chopped I and Q lines to prevent RF pick-up from entering or exiting the box.

Table 3.4  
Connections to Box C2

Signal	Type of Connector
Error In	SMA
Chopped Error Out	BNC
10 KHz In	1500 pf feed-through
10 KHz In	1500 pf feed-through
De-chopped I Out	1500 pf feed-through
De-chopped Q Out	1500 pf feed-through
+15 Volts	1500 pf feed-through
-15 Volts	1500 pf feed-through

#### 3.2.2.1.1 Card 1: ANF Error Signal Chopper

The schematic diagram for this card is given in Figure 3.9. It is identical to Figure 3.6 (the schematic for Box C1, Card 1), except that the PSC2-1 hybrid splitter is not present here, since this box only has to process the feedback error signal for one loop, the Adaptive Notch Filter. In all other respects, the circuit operates the same as Box C1, Card 1, described in Section 3.2.2.1.

#### 3.2.2.1.2 Card 2: ANF 10 KHz Generation and De-chopping

This card is identical to Box C1, Card 2. See Section 3.2.2.2 and Figure 3.7.

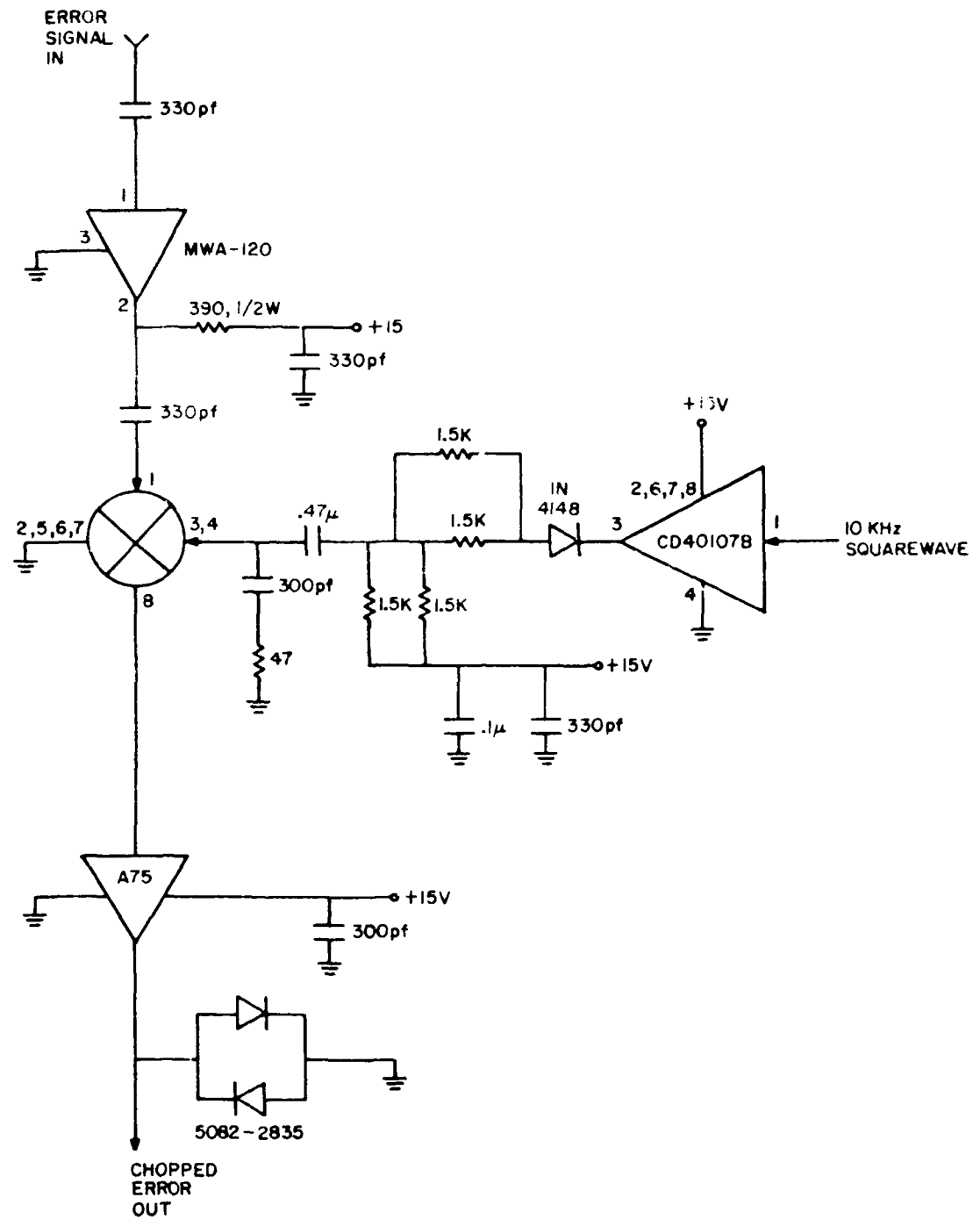


Figure 3.9 Box C2, Card 1: ANF Error Signal Chopper

### 3.2.6 Box L2

This box is identical in construction to Box L1. See Section 3.2.3 and Table 3.3.

#### 3.2.6.1 Card 1: ANF Lowpass Filtering

This card is identical to Box L1, Card 1. See Section 3.2.3.1 and Figure 3.8.

### 3.2.7 Box W3

Table 3.5 lists the connections to Box W3. All connections are made to the lid.

Table 3.5  
Connections to Box W3

Signal	Type of Connector
Mod spectrum In	BNC
Reference In	BNC
Error In	BNC
Modulated I Out	BNC
Modulated Q Out	BNC
100 KHz Out	Multipin Connector, Pin K
10 KHz Out	Multipin Connector, Pin D
Modulated I In	Multipin Connector, Pin F
Modulated Q In	Multipin Connector, Pin E
50 Volts	Multipin Connector, Pin A
10 Volts	Multipin Connector, Pin J
1	Multipin Connector, Pin B

#### 3.2.7.1 Card 1: Sideband ICS Weight and Driver

Figure 3.10 shows the schematic diagram for the I-channel circuitry of this card. Q-channel circuitry is identical. This figure is nearly the same as Figure 3.4, the schematic for the Fundamental ICS Weight and Driver, Box W1, Card 1, but there are several points of difference. The M-spectrum input to the weight is amplified by the MWA-120 prior to entering the 1A0260-3 quadrature hybrid. No directional coupler follows the hybrid. In the Fundamental ICS loop, the coupler at this location extracts a sample to provide a reference input to the correlator. But, due to the pilot control used in the Sideband ICS loop, the correlator reference is extracted at a different point and brought into the box separately.

The final difference is that only the  $I^+$  and  $Q^+$  control signals are supplied to the Sideband card, and the  $I^-$  and  $Q^-$  signals are generated internally. This is done by the HA4605 op amp stage, configured as a unity-gain inverter. Beyond this point, both + and - control signals are present, and operation of the circuit is exactly as described for Box W1, Card 1 in Section 3.2.1.1.

#### 3.2.7.2 Card 2: Sideband ICS Correlator, 85 KHz Amplification and Lowpass Filtering

The schematic diagram for the correlator and 85 KHz amplifier portions of this card is presented in Figure 3.11a. The error signal input to the correlator, containing any uncanceled residue of the pilot sidebands, enters and is split by the PSC2-1 hybrid. The reference input to the correlator, tapped off from the transmitter prior to pilot insertion and therefore free of any pilot sidebands, enters the 1A0260-3 quadrature hybrid which separates it into I and Q components. From this point on, I-channel and Q-channel circuits are identical, and only the I side is shown.



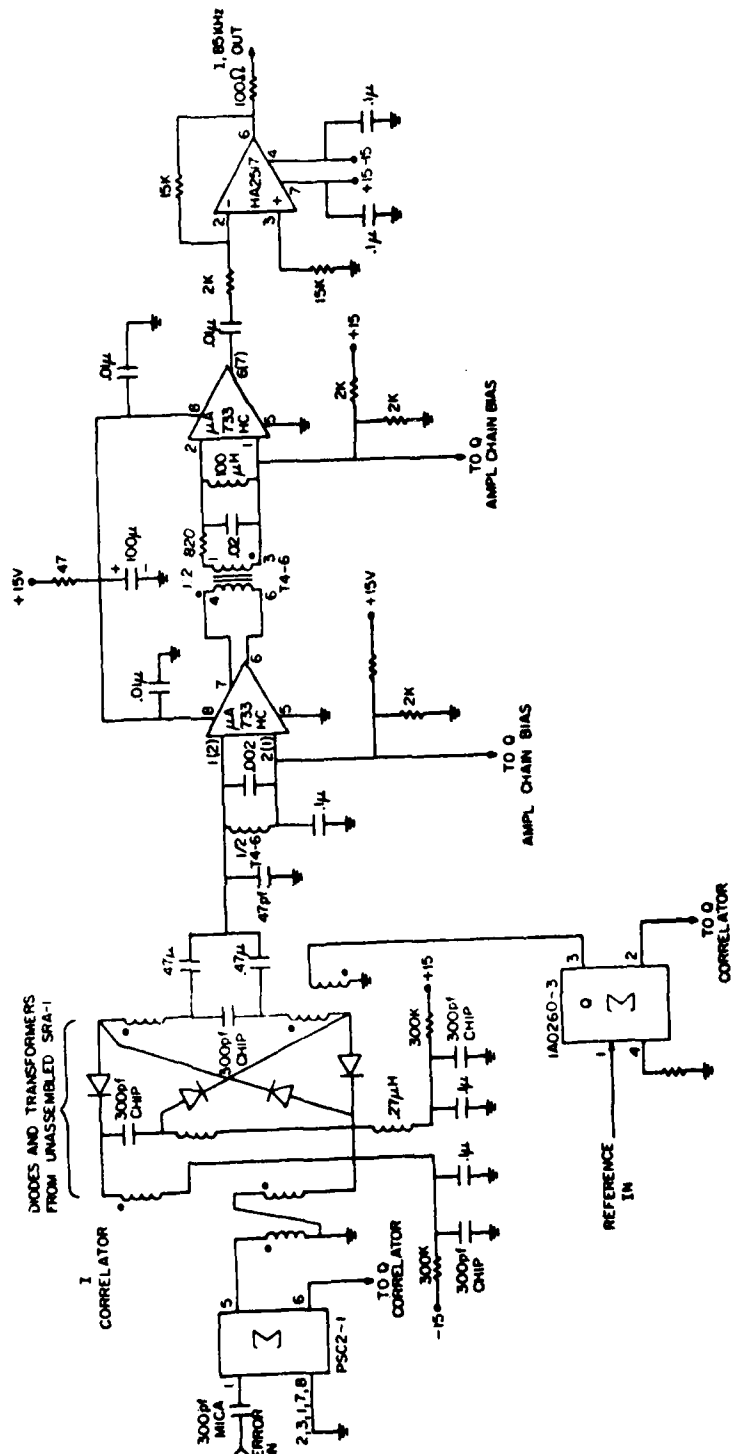


Figure 3.11a Box W3, Card 2: Sideband ICS Correlator and 85 KHz Amplification

The correlator is implemented as in Boxes W1 and W2, a diode quad double-balanced mixer with a small DC current applied to the diodes. However, for the Sideband ICS, the correlator output is at the pilot frequency, 85 KHz. Amplification of the 85 KHz signal is accomplished by two stages of  $\mu$ A733 video amplifiers, coupled by the T4-6 transformer. Each of the 733s has an 85 KHz bandpass network at the input to reject harmonics of the pilot frequency. Final amplification is by the HA2517 op amp. The output of the 2517 leaves the box to go to the Pilot Demodulator.

This card also contains the lowpass filters for the Sideband ICS loop. Figure 3.11b gives the schematics for the I-channel circuitry. Q-channel circuitry is identical. The demodulated I (or Q) control signal enters the HA4741 op amp, configured as a lowpass filter with a 1.7 Hz corner frequency and 26 dB DC gain. As in the other LPF circuits, speed-up diodes have been included to provide higher gain during acquisition. The 10 K pot is used to adjust out DC offsets. The 100  $\mu$ f decoupling capacitors at each end of the pot prevent 60 Kz power supply ripple from entering the control lines. Diagnostic jacks are provided at the outputs of the lowpass filters.

#### 3.2.8 Box P

Table 3.6 lists the signal interfaces for Box P. Feed-through connectors (1500 pf) are used for the +15 and -15 volt supply lines, 85 KHz I and Q lines, and demodulated I and Q lines to prevent RF pick-up from entering or exiting the box.

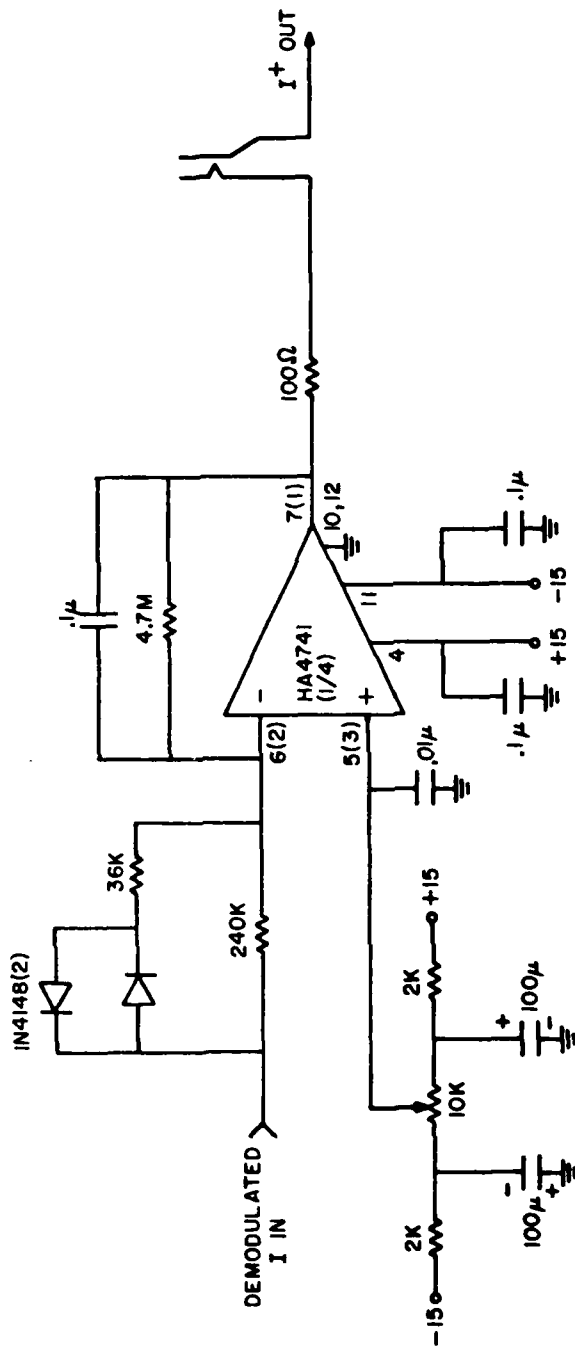


Figure 3.11b Box W3, Card 2: Lowpass Filtering

Table 3.6  
Connections to Box P

Signal	Type of Connector
Transmitter Signal In	BNC
Transmitter Signal + Pilot Out	BNC
I 85 KHz In	1500 pf feed-through
Q 85 KHz In	1500 pf feed-through
Demodulated I Out	1500 pf feed-through
Demodulated Q Out	1500 pf feed-through
+15 Volts	1500 pf feed-through
-15 Volts	1500 pf feed-through

#### 3.2.8.1 Card 1: Pilot Modulator

The Pilot Modulator is used to introduce pilot sidebands on the transmitter waveform at the pilot frequency, 85 KHz. Its schematic is presented in Figure 3.12. A sample of the transmitter signal is extracted by the first 20 dB directional coupler (PDC20-1). This sample goes through a 20 dB attenuator, then into a SRA-1 mixer, where it gets DSB modulated by the  $\sin \omega_p t$  output of the 85 KHz Pilot Oscillator, brought in from Card 2 of this box. The sidebands produced are amplified in the MWA-120, then injected back on to the main line through the second 20 dB coupler (PDC20-1). The MWA-120 amplifier helps to isolate the mixer from backward-traveling signals that might leak through the second coupler.

#### 3.2.8.2 Card 2: Pilot Oscillator and Demodulator

The schematic diagram for this card is shown in Figure 3.13. The XR2206 function generator serves as the oscillator. Both outputs of the XR2206 are used: Pin 2 is the  $\sin \omega_p t$  output of the chip, used by the Pilot Modulator on Card 1; Pin 11 is a squarewave output whose phase is that of  $\cos \omega_p t$ . This squarewave is the signal supplied to the demodu-

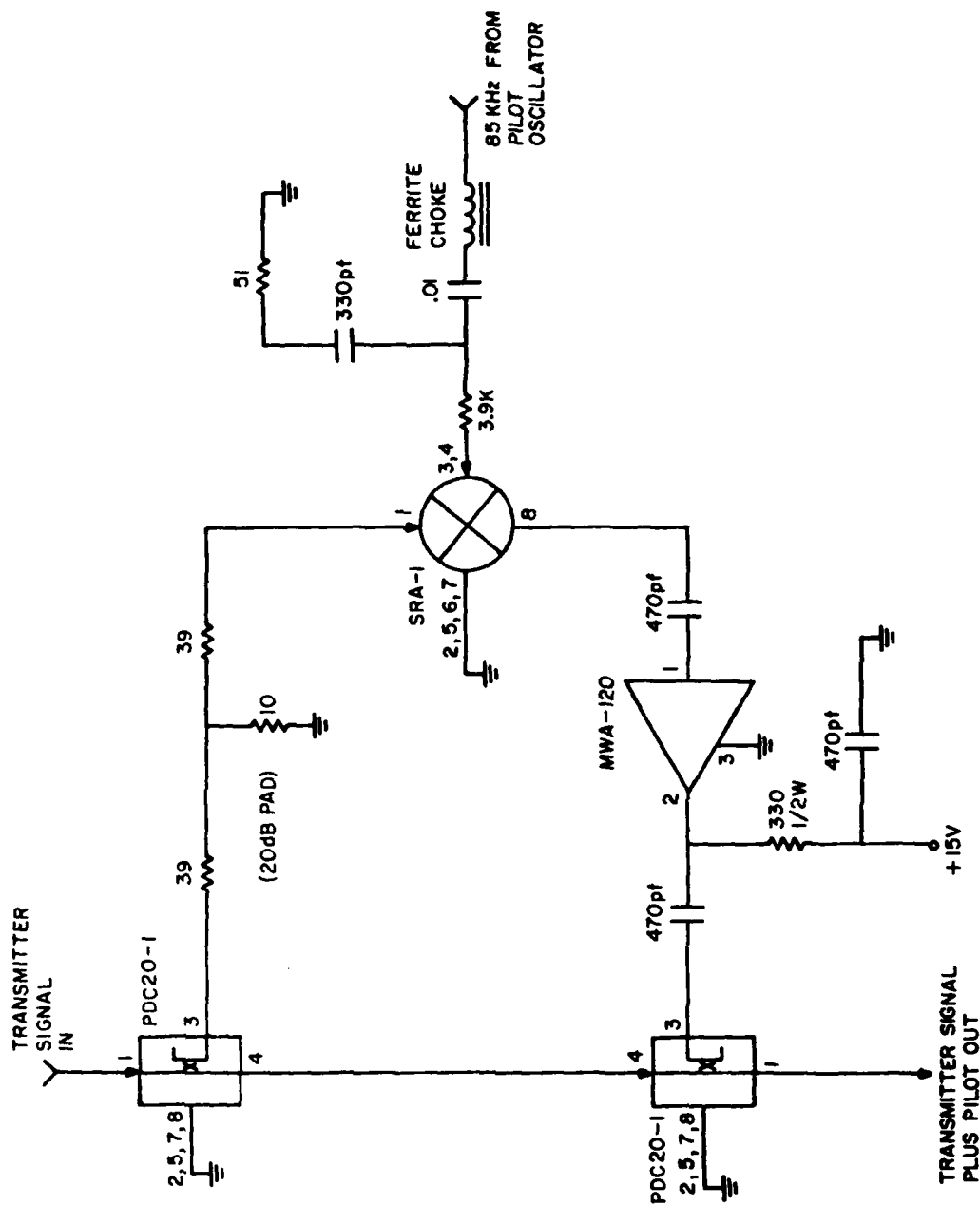


Figure 3.12 Box P, Card 1: Pilot Modulator

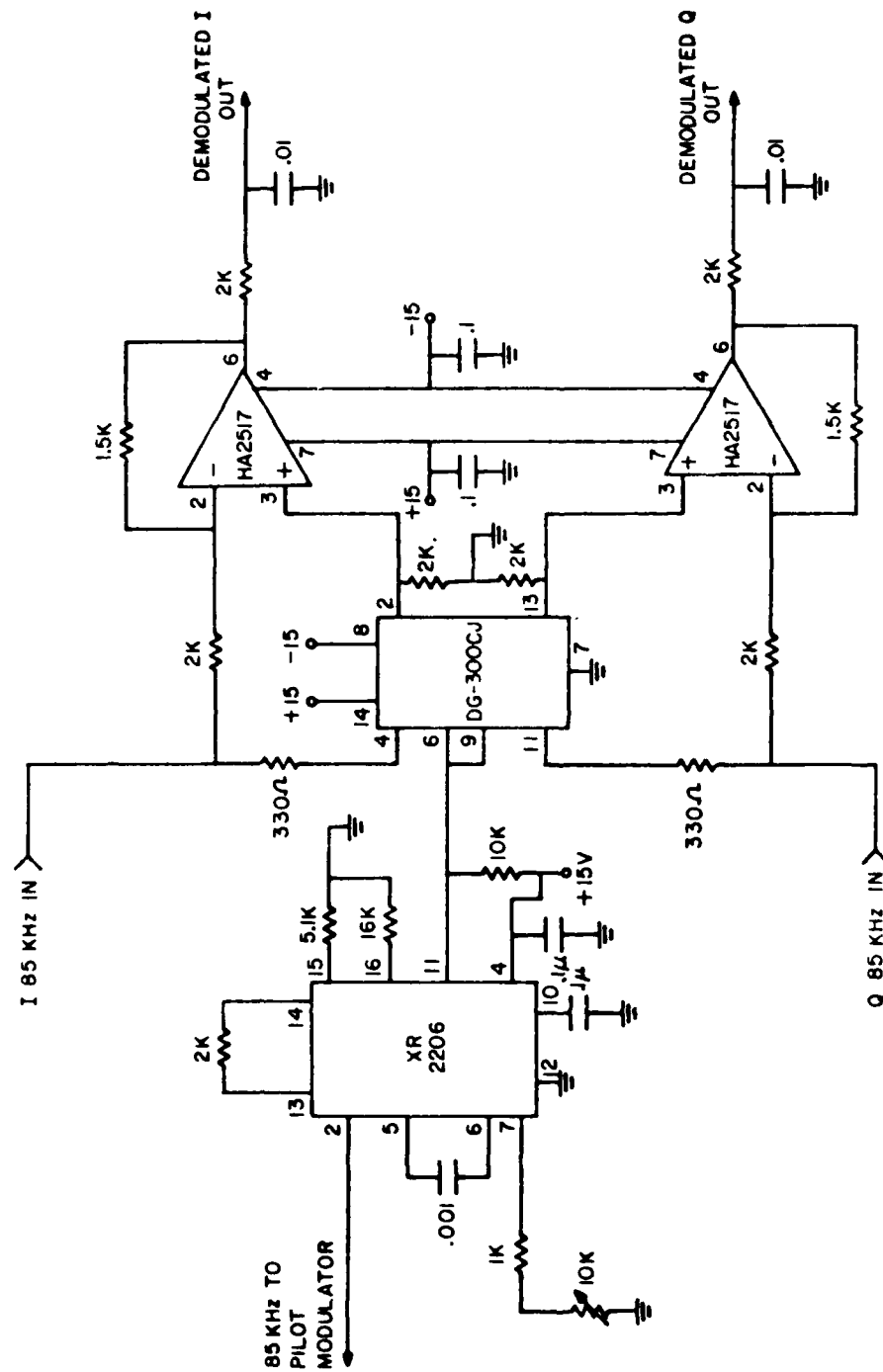


Figure 3.13 Box P, Card 2: Pilot Oscillator and Demodulator

lator.

The demodulator circuitry is nearly identical to the de-choppers in Boxes C1 and C2. The DG300 analog switch, controlled by the 85 KHz pilot squarewave, alternately flips the configuration of the HA2517 op amps between inverting and non-inverting modes, creating a full-wave synchronous detector.

#### 4.0 OPERATING NOTES

The BBICS unit is designed to operate in a laboratory environment. Prime power is 120 volt, 60 Hz, single phase. Two 2-amp fuses are provided, accessible from the front panel.

The Pilot Modulator provided was designed for low-power demonstration purposes only, and cannot handle a full range of typical transmitter power levels. Power into the "PILOT MODULATOR--RF IN" port should not exceed 3 watts.

The connection between the "PILOT MODULATOR--RF OUT" port and the "REFERENCE INPUT" port forms part of the error signal path to the Sideband ICS correlator. Hence it must be matched in delay with the reference signal path to the correlator. To achieve this, the cables and couplers used to connect the two ports must have a total delay equivalent to 19 inches of RG-188 cable.

The power level supplied to the "REFERENCE INPUT" port should be +33 dBm to ensure proper gain in the ICS loops. The interference power level at the "MAIN INPUT" port must be at least 13 dB lower than the level at the "REFERENCE INPUT" port to guarantee that the BBICS will be able to cancel the interference even under worst-case insertion loss conditions.

Figure 4.1 shows a typical experimental configuration in which the BBICS might be used. A signal generator and power amplifier are used to simulate the interfering transmitter. A bandpass filter at the interference frequency is included to eliminate harmonics generated in the power amp. The cables used to connect the "PILOT MODULATOR--RF OUT" port to the "REFERENCE INPUT" port are selected so that the total electrical length, including the straight-through path of the directional coupler, approximates 19 inches of RG-188. Power level of the signal generator is adjusted so that the power entering the "REFERENCE INPUT" port is +33 dBm.

The interference coupling path is simulated by tapping off the "PILOT MODULATOR--RF OUT" line with a 10 dB directional coupler, followed by 3 dB additional attenuation and some arbitrary length of delay line. The

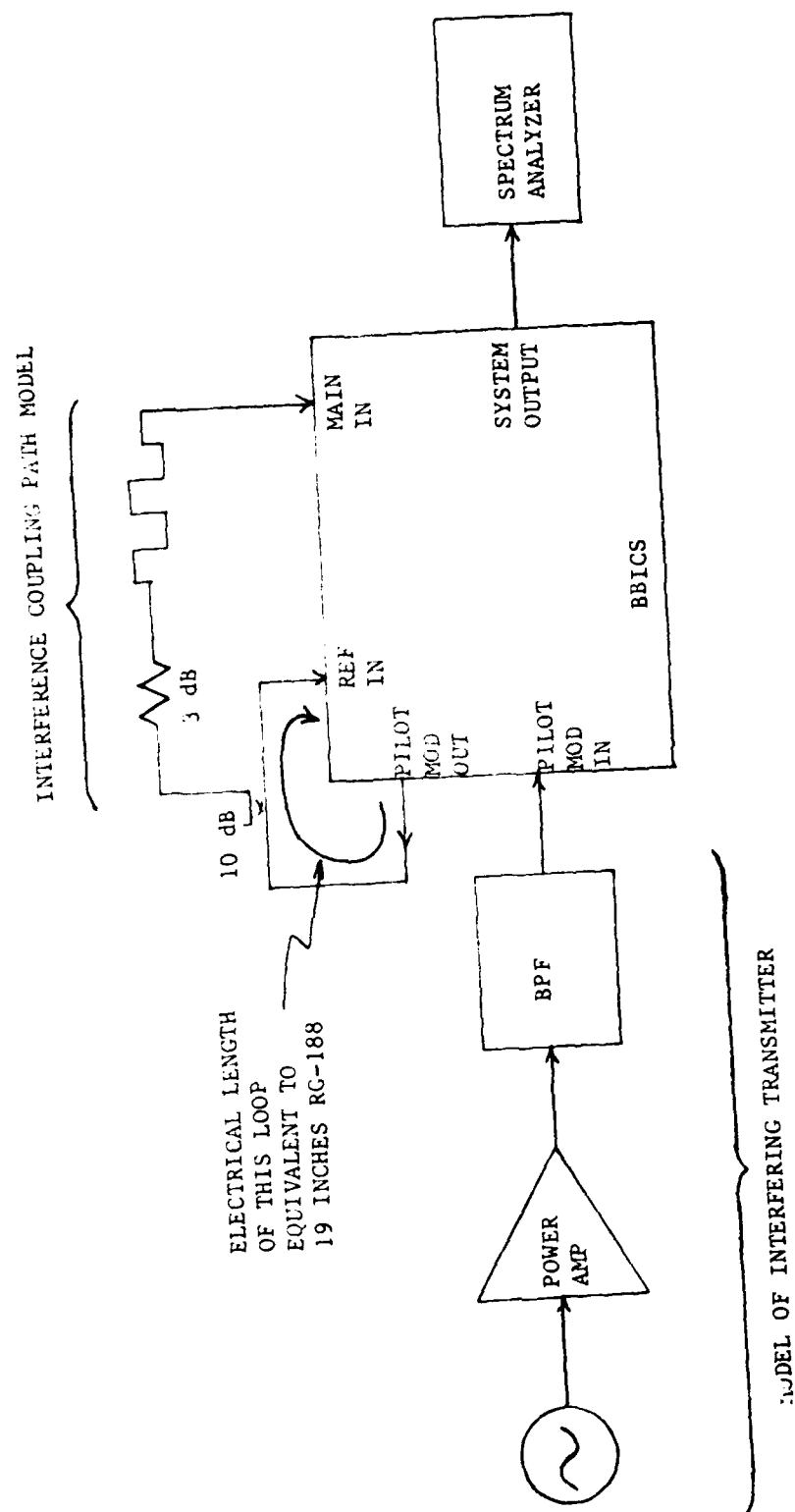


Figure 4.1 Typical BBICS Experimental Configuration

combination of the 10 dB coupler and the 3 dB pad ensures that the interference power level entering the "MAIN INPUT" port is at least 13 dB below the +33 dBm level entering the "REFERENCE INPUT" port. The 3 dB pad could be omitted if a long delay line having more than 3 dB intrinsic loss were being used.

A spectrum analyzer is shown positioned to monitor the system output. In some cases, an amplifier may precede the analyzer to allow viewing of extremely low-level signals.

## 5.0 SYSTEM PERFORMANCE

A series of experiments were conducted to evaluate the performance of the BBICS system described in the previous chapter. Testing was concentrated in three areas:  $f_o$  cancellation, sideband cancellation, and acquisition time. Results of these performance tests are presented below.

### 5.1 $f_o$ Cancellation

This first set of measurements concerns the cancellation of a single tone interference. Figure 5.1 shows the experimental set-up used in making the measurements. The interfering tone at  $f_o$  comes from the signal generator and is amplified by the RF power amp. The bandpass filter is present to reject harmonics of  $f_o$ .

Three different channel models were used to simulate possible interference coupling paths between transmitter and receiver. These models are designated as follows: "No Cable" indicates that there was no connection supplied to the main input; "Short Cable" indicates a 10 dB directional coupler off the reference path, followed by 2 dB additional attenuation and 4 feet of RG-58 cable leading to the main input; and "Long Cable" refers to the 10 dB coupler off the reference path followed by 50 feet of RG-58. (This cable length was chosen to provide the same sideband cancellation residue in a single loop ICS as would be obtained using the multipath coupling channel model developed by RADC for the B-52 aircraft.

Table 5.1 lists the cancelled and uncanceled power levels measured at the system output. Uncanceled levels were obtained by disconnecting the reference input to the BBICS.

Table 5.1 System Output Power at  $f_o$

$f_o$ Frequency	No Cable Cancelled	Short Cable		Long Cable	
		Uncanceled	Cancelled	Uncanceled	Cancelled
225 MHz	-52 dBm	+12 dBm	-49 dBm	+12 dBm	-50 dBm
250	-50	+ 9	-49	+10	-50
275	-50	+12	-49	+11	-54

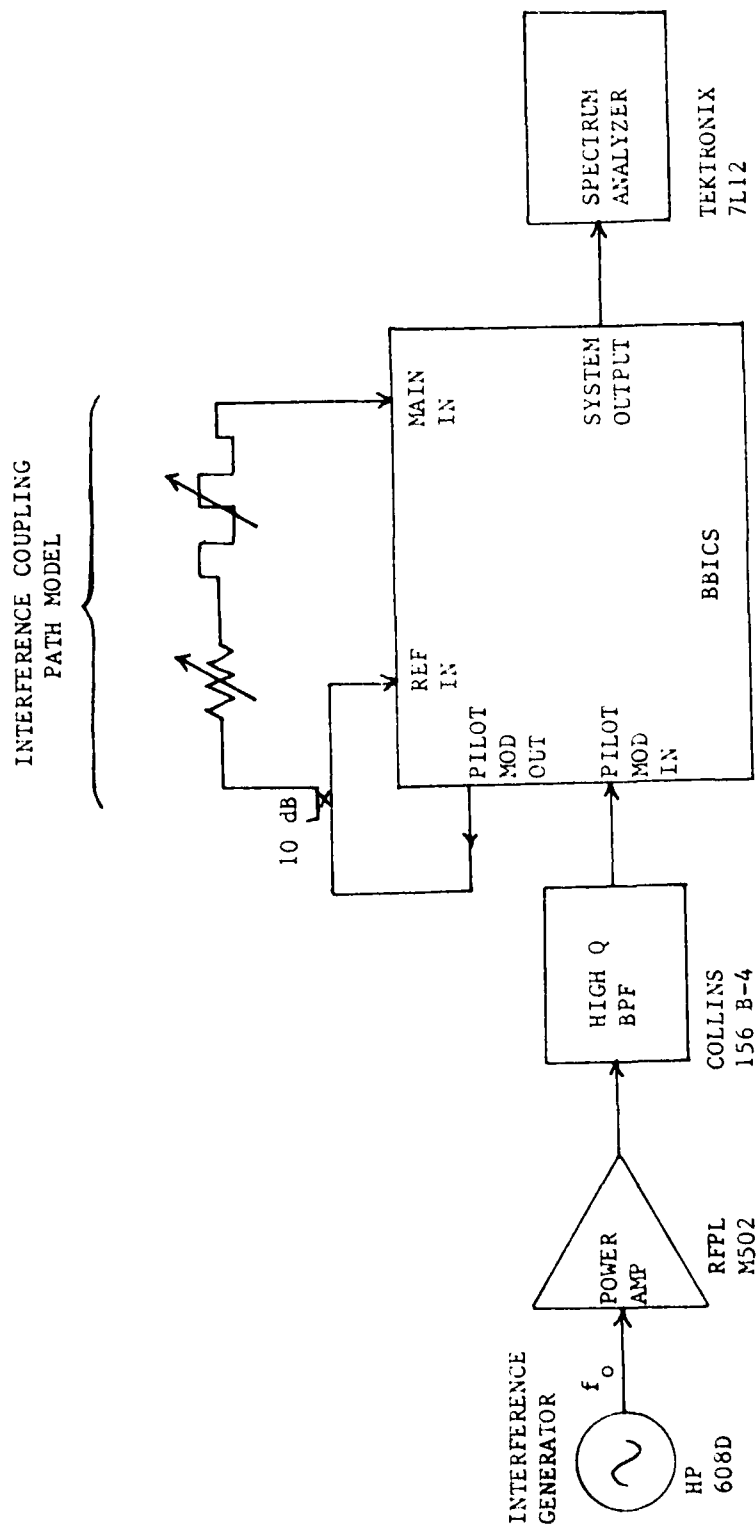


Figure 5.1 Experimental Set-up to Measure  $f_o$  Cancellation

Table 5.1 (cont.)

$f_o$ Frequency	No Cable Cancelled	Short Cable		Long Cable	
		Uncancelled	Cancelled	Uncancelled	Cancelled
300 MHz	-49 dBm	+10 dBm	-46 dBm	+10 dBm	-49 dBm
325 *	-40	+13	-40	+12	-40
350	-54	+11	-50	+10	-53
375	-49	+10	-48	+ 9	-49
400	-48	+10	-48	+10	-46

## 5.2 Sideband Cancellation

As explained earlier during the discussion of system concept, noise sidebands present on the interfering waveform will be cancelled by the BBICS in exactly the same manner as the 85 KHz pilot sidebands that the system adds to the interference. Thus we can conveniently measure noise sideband cancellation by determining the cancellation achieved on the pilot sidebands directly. This was done using the same experimental set-up used for  $f_o$  cancellation (Figure 5.1), except that a TRW CA2820 30 dB amplifier was inserted ahead of the spectrum analyzer in order to magnify the output sideband levels enough to make them visible.

Table 5.2 lists the cancelled and uncancelled sideband power levels measured at the system output. The three channel models used to simulate the interference coupling path are the same ones used in the previous section.

Table 5.2 Output Power in Pilot Sidebands

$f_o$ Frequency	No Cable Cancelled	Short Cable		Long Cable	
		Uncancelled	Cancelled	Uncancelled	Cancelled
225 MHz	-108 dBm	-44 dBm	- 96 dBm	-44 dBm	-100 dBm
250	-104	-46	-100	-45	-100
275	-107	-43	-105	-44	-101
300	-100	-46	- 97	-47	- 97
325 *	- 97	-45	- 97	-45	- 95

\* Unexplained anomalous data points at this frequency.

Table 5.2 (cont.)

$f_o$ Frequency	No Cable Cancelled	Short Cable		Long Cable	
		Uncancelled	Cancelled	Uncancelled	Cancelled
350 MHz	-100 dBm	-46 dBm	-100 dBm	-48 dBm	- 99 dBm
375	-100	-48	-102	-50	-104
400	-102	-49	-102	-50	- 98

In order to verify the assertion that cancellation of the pilot sidebands implies cancellation of transmitter noise sidebands, the experimental set-up shown in Figure 5.2 was implemented. The probe generator puts out a wideband (about 200 KHz) FM spectrum centered about the same fundamental frequency as the interference generator. The two signals combine in the directional coupler to simulate a transmitter waveform with strong noise sidebands. Figure 5.3 shows spectrum analyzer photographs of the BBICS operating on this interference model. Center frequency was 300 MHz, and the "Long Cable" coupling path simulator was used. Figure 5.3a shows the uncanceled system output, achieved by disconnecting the reference input. The spectrum analyzer is not preceded by the 30 dB amplifier for the uncanceled measurement, so that the top line on the display is truly +20 dBm. Note then that the uncanceled  $f_o$  power level is +14 dBm, and the uncanceled sideband levels at the edges of the screen are approximately -47 dBm. The sidebands at 30 KHz away from  $f_o$  are modulation products produced by a spurious signal inside the analyzer and should be ignored.

Photo b in Figure 5.3 is the cancelled system output with only the fundamental ICS loop operating (the sideband loop has been disconnected). The 30 dB amplifier is now in place ahead of the spectrum analyzer, so that the top line on the display actually corresponds to -50 dBm, not -20 dBm. The  $f_o$  power level is seen to be -57 dBm, indicating 71 dB of  $f_o$  cancellation. The sideband height at the screen's edge is -77 dBm, showing only about 30 dB of sideband cancellation. This is the expected result of the M-effect for a single-loop ICS.

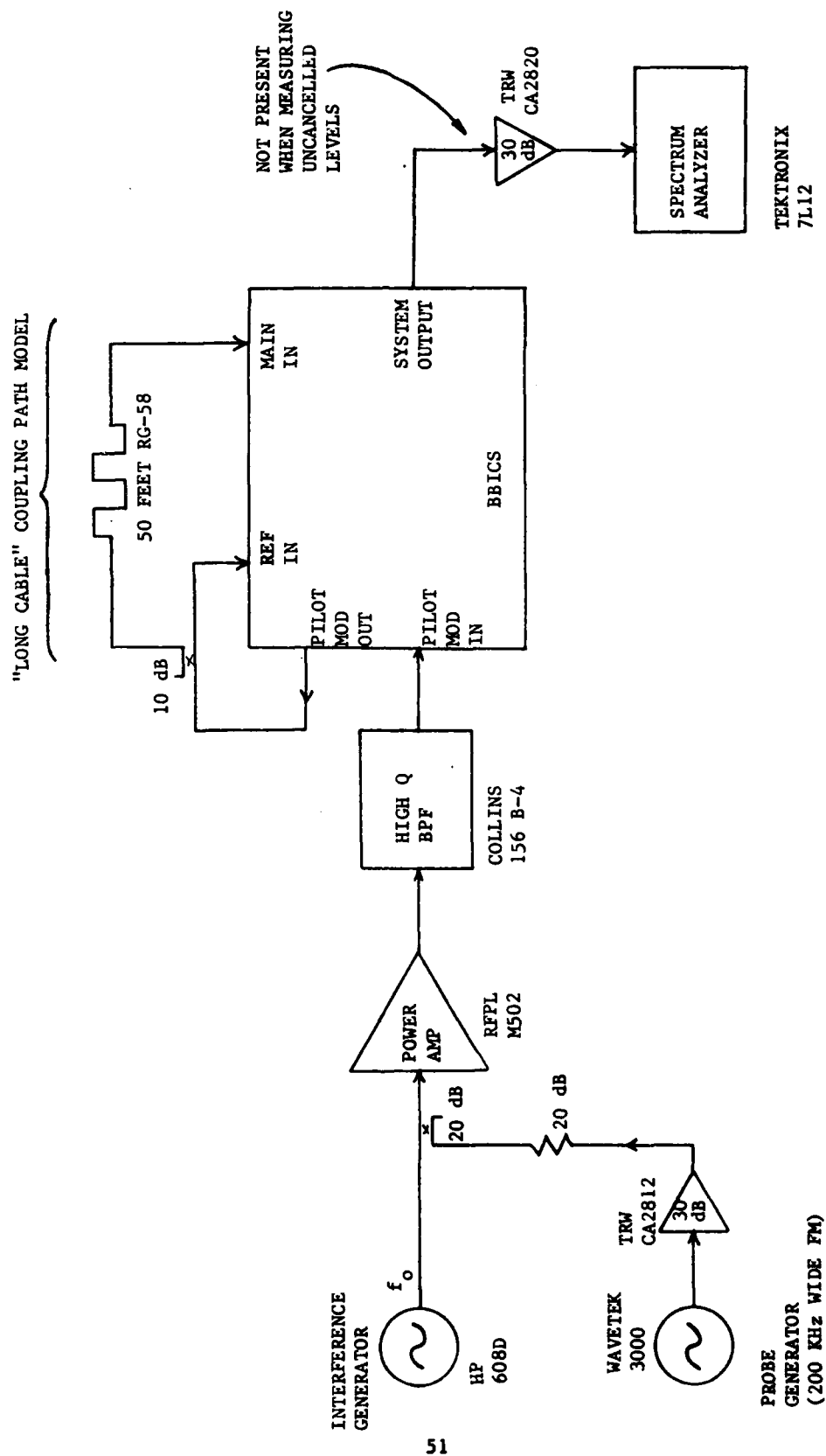
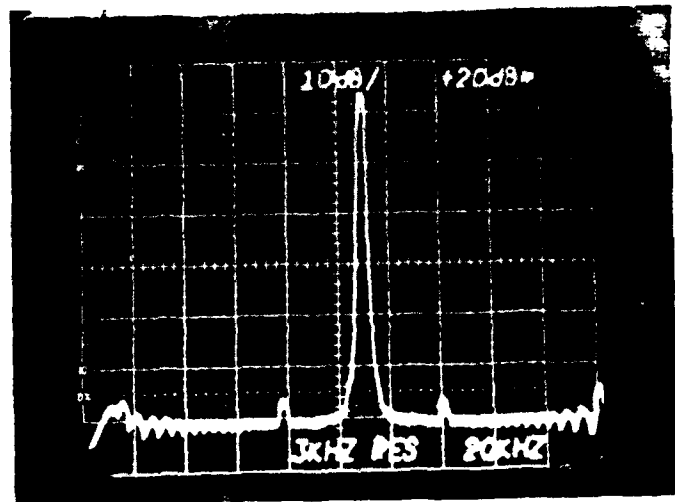


Figure 5.2 Experimental Set-up to Observe Noise Sideband Cancellation

### 5.3a Uncancelled System Output

Horizontal Scale: 20 KHz per division

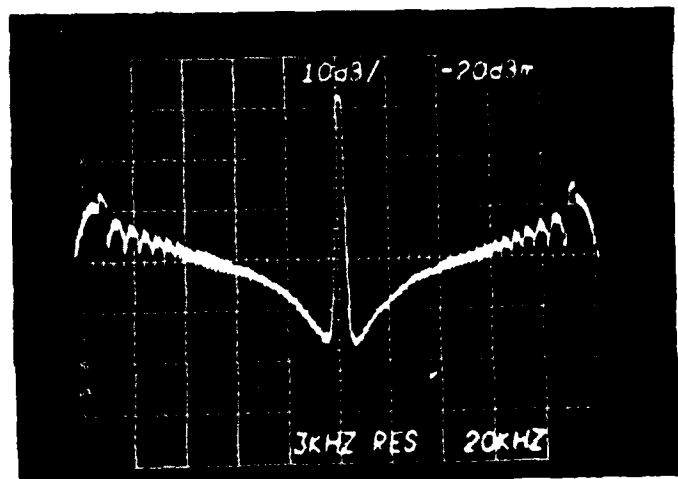
Vertical Scale: +20 dBm top line,  
10 dB per division



### 5.3b Cancelled System Output with One Channel Operating

Horizontal Scale: 20 KHz per division

Vertical Scale: -50 dBm top line,  
10 dB per division



### 5.3c Cancelled System Output with Both Channels Operating

Horizontal Scale: 20 KHz per division

Vertical Scale: -50 dBm top line,  
10 dB per division

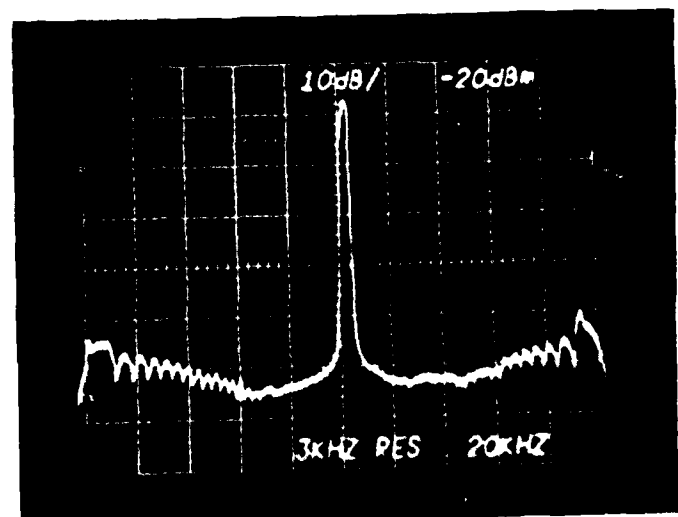


Figure 5.3 BBICS Performance Against an Interference Consisting of a Strong  $f_0$  Component (300 MHz) Plus Wideband FM Sidebands

Photo c shows the cancelled system output with both BBICS loops operating. The cancelled  $f_o$  level is unchanged from photo b. But sideband cancellation has improved significantly. Edge-of-screen levels are approximately -103 dBm, indicating 56 dB of sideband cancellation.

### 5.3 Acquisition Time

Figure 5.4 shows the experimental set-up used to measure acquisition time, which is being defined as the time the ICS takes to reach steady state from the moment the interfering transmitter is turned on. To simulate transmitter turn-on, the ZAY-3 double-balanced mixer is used as an RF switch, activated by manual triggering of the pulse generator. The spectrum analyzer is operated as a fixed-tuned receiver at  $f_o$ , so that it displays power at  $f_o$  versus time. By using the same pulse that switches the RF to trigger the analyzer sweep, the display can be used to monitor the time it takes the BBICS to cancel the large  $f_o$  component of the interference.

Cancellation of the sidebands cannot be observed so directly. But the I and Q weight control voltages for the sideband ICS loop can be accessed easily and monitored on an oscilloscope. The pulse that switches the RF and triggers the spectrum analyzer can be used to simultaneously trigger the oscilloscope sweep. When the I and Q control voltages reach constant values, the sideband loop has reached steady state, and sideband cancellation has been achieved.

Figure 5.5 is a photograph showing the results of the acquisition time measurement for  $f_o = 300$  MHz. The photo shows three traces: the spectrum analyzer display of power at  $f_o$  vs. time, and the two oscilloscope traces of I and Q control volts vs. time. Cancellation time for  $f_o$  is seen to be approximately 7 msec. Sideband cancellation does not begin until  $f_o$  cancellation is completed, and ends when the control voltages level off, roughly 19 msec after transmitter turn-on.

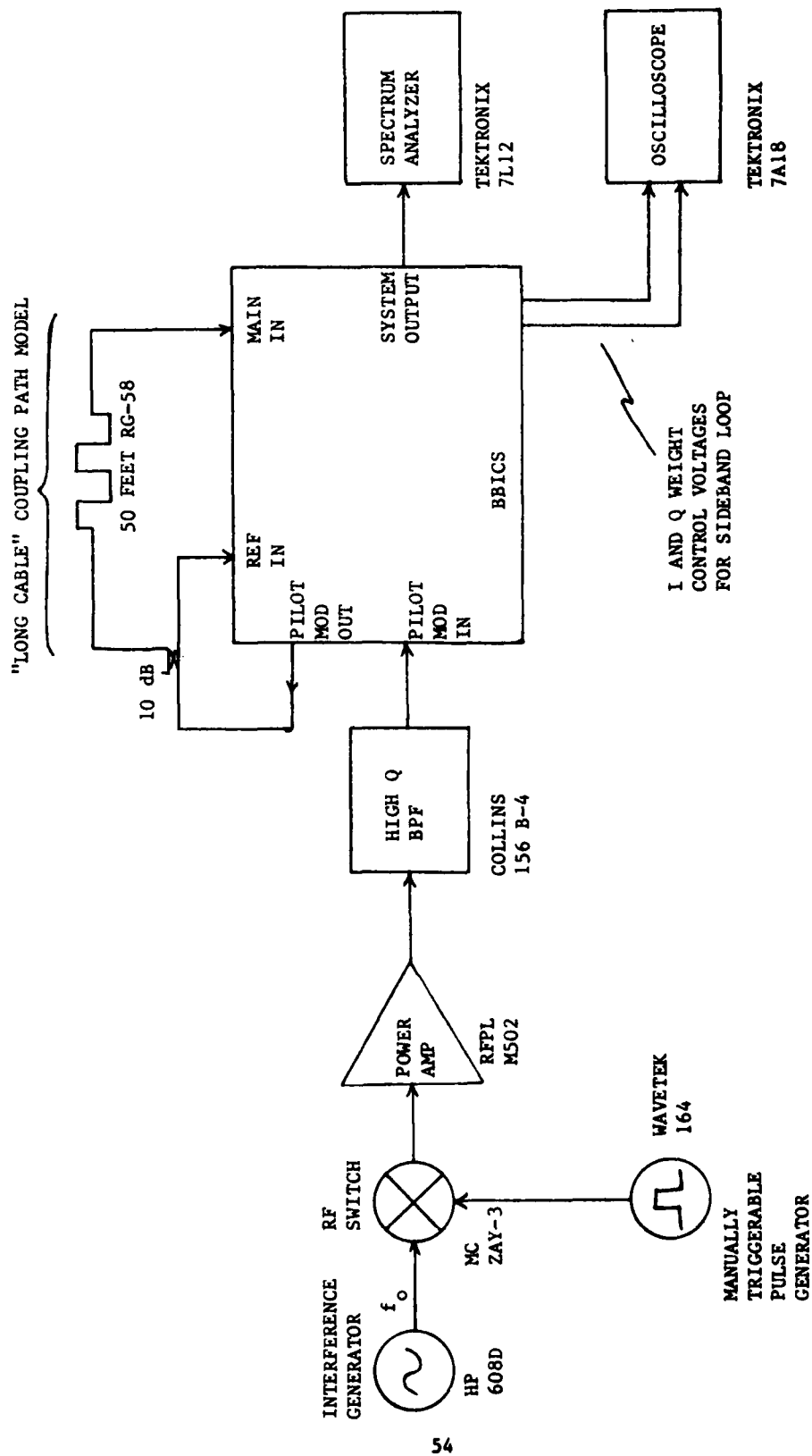
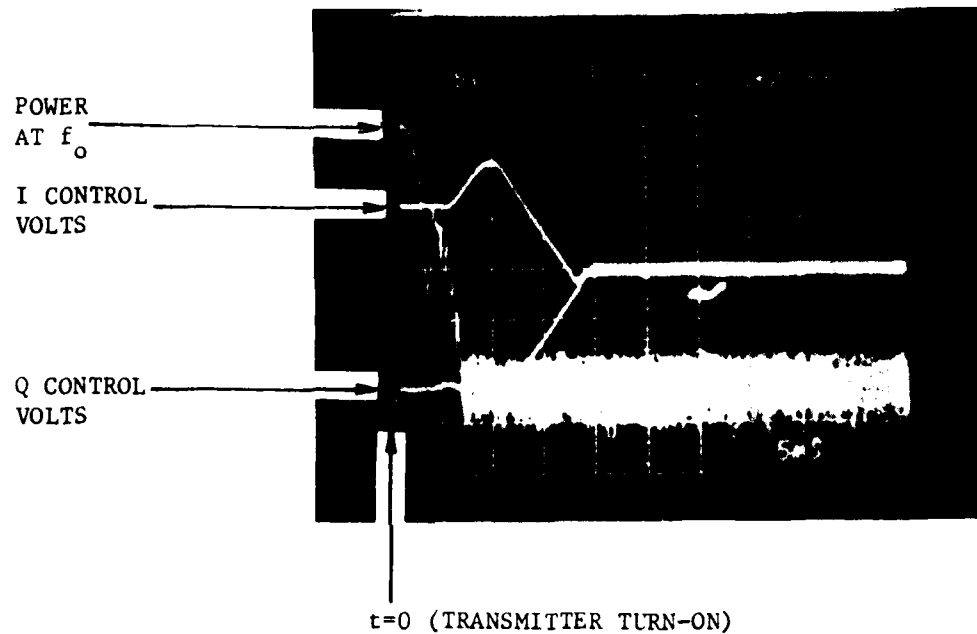


Figure 5.4 Experimental Set-up to Measure Acquisition Time



Horizontal Scale: 5 msec per division

Vertical Scales:

Power at  $f_0$ : +20 dBm top line,  
10 dB per division

I and Q control volts: 5 volts per division

Figure 5.5 Acquisition Time Behavior at  $f_0 = 300$  MHz

## 6.0 CONCLUSIONS AND RECOMMENDATIONS

The concept has been presented for a two-channel ICS which provides improved broadband cancellation compared to that achievable with a single-channel ICS. The input to the second-channel weight is spectrally pre-shaped by an adaptive notch filter which automatically tracks the frequency of the interference. Control of the second-channel weight utilizes a novel pilot-directed control system.

A functioning unit was constructed to implement the design concept. Experimental measurements of the unit's performance showed enhanced broadband cancellation of the order expected, and verified that the system concept and design were sound.

Future efforts should be directed towards improving the system to use a weaker pilot signal, or a pilot which is more spectrally spread out. Also, the Pilot Modulator's power-handling ability should be increased, say to 100 watts, so that the system can be tested with standard transmitter sets. The present Pilot Modulator, intended for demonstrations with low-power laboratory test equipment, has a 3 watt maximum power limitation.

More extensive testing of the BBICS should include using RADC's simulated multipath coupling channel for the B-52 aircraft as the experimental interference coupling path. Eventually the unit's performance should be tested in an aircraft environment.

#### REFERENCES

- [1] B.S. Abrams, et al, "Interference Cancellation," General Atronics Corp. Final Report RADC-TR-74-225, September 1974.
- [2] M.J. Di Toro, "Communication in Time-Frequency Spread Media Using Adaptive Equalization," Proc. of the IEEE, Vol. 56, October 1968, pp. 1653-1679.
- [3] P.A. Bello, "Characterization of Randomly Time-Variant Linear Channels," IEEE Trans. Comm. Systems, Vol. CS-11, December 1963, pp. 360-393.
- [4] B. Widrow, et al, "Adaptive Antenna Systems," Proc. of the IEEE, Vol. 55, No. 12, December 1967, pp. 2143-2159.
- [5] B.S. Abrams, et al, "Adaptive Same Frequency Repeater (SFR) Study," General Atronics Corp. Final Report RADC-TR-76-78, March 1976.

DATE  
FILMED  
8